Analog models of the lateral spreading of a thick three-layer crust –

Implications for the Svecofennian orogen in Finland

Kaisa Nikkilä

Åbo Akademi University

Geology and Mineralogy
Faculty of Science and Engineering
Åbo Akademi University
Åbo, Finland, 2016

ANALOG MODELS OF THE LATERAL SPREADING OF A THICK THREE-LAYER CRUST –

IMPLICATIONS FOR THE SVECOFENNIAN OROGEN IN FINLAND

Kaisa Nikkilä

ACADEMIC DISSERTATION

Geology and Mineralogy
Faculty of Science and Engineering
Åbo Akademi University
Åbo, Finland, 2016

“In a dark place we find ourselves, and a little
more knowledge lights our way.”

— Yoda

Supervisors

Professor Olav Eklund
Geology and Mineralogy
Faculty of Science and Engineering
Åbo Akademi University
Domkyrkotorget 1, 20500 Åbo
Finland

Docent Annakaisa Korja
Institute of Seismology
Department of Geosciences and Geography
University of Helsinki, 00014 Helsinki
Finland

Reviewers

Dr. Giacomo Corti
Tectonic Modeling Laboratory
National Research Council of Italy
Via G. La Pira 4, 50121 Florence,
Italy

Dr. Taija Torvela
School of Earth and Environment
University of Leeds, LS2 9JT Leeds
United Kingdom

Opponent

Dr. Giacomo Corti
Tectonic Modeling Laboratory
National Research Council of Italy
Via G. La Pira 4, 50121 Florence,
Italy

Layout: Pia Sonck-Koota / www.sonck-koota.fi
ISBN 978-952-12-3429-3 (printed)
ISBN 978-952-12-3430-9 (pdf)
Painosalama Oy – Turku, Finland 2016

Abstract

Our knowledge of the crustal structure of the Precambrian Svecofennian orogen has been enhanced during the last decade. Much of the new knowledge is due to the deep seismic reflection studies (Finnish Reflection Experiments; FIRE), which transect the main lithological units and tectonic boundaries on the Finnish side of the Fennoscandian Shield, showing a frozen image of the crustal structure. Understanding of the crustal structures improves interpretations of crustal evolution. However, the tectonic events and processes causing the anomalies/structures cannot be directly defined from the profiles. The processes can be studied by analog modeling, which is a viable tool for filling in absent components of a puzzle of reconstruction of the crustal evolution. The analog modeling can yield information on the generation and the development of crustal scale structures and crustal components, for example, after mountain building process. In this thesis, post-accretion crustal evolution of thickened orogenic crust is studied via analog modeling. Geochronological, geochemical and geophysical data from the central part of the Svecofennian orogen are used to compare analog models to nature.

The thesis presents two sets of analog modeling experiments, thermomechanical and centrifuge, which are simulating the lateral spreading of a three-layer crust after thermal relaxation. In the modeling experiments, it is assumed that the spreading is caused by the differences in gravitational potential energy between the thickened orogenic crust and the adjacent thinner areas. In the experiments, the spreading is dictated towards free space. In the centrifuge modeling, the spreading is gravitationally induced and produces lateral flow and ductile uplift. In the thermomechanical modeling, the spreading is thermally induced and it only produces lateral flow.

The analog modeling results show that a thick accretional orogenic crust with ductile middle layer will undergo lateral and gravitational spreading in all crustal layers. The spreading results in subsiding of upper and middle crusts, uplifting of lower and middle crusts; thinning, thickening and elongation of middle and lower crusts; and crustal scale block rotation. The lateral spreading can also result in reverse faults and shortening of layers and blocks, although the extensional structures are predominant. The lateral spreading rotates tectonic boundaries towards the spreading direction by elongating and shortening those. The deformation is most dominant in the ductile middle layer. In the models where tectonic boundaries are present, the spreading is accommodated on both sides of the boundary zones indicating that a crust, undergoing gravitational spreading, suffers from deformation across the orogenic belt.

The geophysical data – aeromagnetic, seismic reflection and refraction data – from the central part of the Svecofennian orogen have shown that the orogenic belt is composed of fragmental crustal blocks separated by large-

scale shear zones. The comparison to analog models suggests that the crustal scale shear zones and the wide bands of high reflectivity in seismic profiles are reactivated terrane boundaries and thick-skin stacking surfaces, which have elongated and rotated westward.

Geochronological, geochemical and structural data from the Paleoproterozoic Central Finland granitoid complex show that the plutons have been emplaced at a post-accretion stage during middle crustal exhumation and lateral spreading. The exhumation and the lateral spreading started at ca. 1884 Ma and continued until 1870 Ma. The rocks can be divided into three groups by their geochemical and geochronological characteristics. Group 1 rocks have formed from melts from the lower crust and have been emplaced >1887 Ma to the upper and the middle crusts. Group 2 rocks have formed from melts from the middle crust and have been emplaced at 1890-1886 Ma and at 1884-1883 Ma to (sub)surface and to the upper part of the middle crust, respectively. Group 3 rocks have formed from melts from the lower crust and they have been emplaced at 1881-1880 Ma in the upper parts of the middle crust. Each magma group represents an important event in the crustal evolution: the Group 1 magmas are the first post-accretion melts of the thickened crust, the Group 2 magmas are the result of widespread middle crustal melting due to thermal relaxation, and the Group 3 magmas are emplaced during extensional event. The ongoing exhumation between 1884 Ma and 1870 Ma changed the deformation style of the plutonic rocks from pervasive foliation to localized shear zones. The comparison between the CFGC and the adjacent areas shows that the coeval deformation and magmatism are present in the entire central part of the orogen.

Furthermore, the analog models and the data from the central part of the Svecofennian orogen in Finland suggest that the coeval exhumation, the lateral spreading and changes in the magma type across the orogen can be explained by westward gravitational spreading.

Sammanfattning

Vår kuskap om jordskorpans stora strukturer, som bildats under den Prekambriska Svekofenniska orogenesen, har under det senaste årtiondet ökat avsevärt. En stor del av de nya kunskaperna har förbättrats tack vare reflektionsseismisk forskning (Finnish Reflection Experiments; FIRE). De seismiska FIRE profilerna visar en frusen bild av jordskorpans strukturer. Bilderna visar hur de viktigaste litologiska enheterna skär varandra och olika tektoniska enheter på den finska sidan av Fennoskandiska skölden. De tektoniska processer som orsakat strukturerna kan inte direkt tolkas från profilerna. Processerna bakom strukturerna kan däremot studeras med analoga modelleringar. Fördelen med analoga modelleringsexperiment är att man kan lägga till komponenter och faktorer som styr jordskorpans evolution, men som inte kan identifieras med andra metoder.

Syftet med denna avhandling är att förstå utvecklingen av en jordskorpa som förtjockats genom ackretionstektonik och därefter tunnats ut (under post-ackretionsskedet), med hjälp av analoga modelleringar. Förutom analoga modeller har geokronologiska, geokemiska och geofysiska data från den centrala delen av den Svekofenniska orogenesen använts för att jämföra analoga modeller med naturen.

Avhandlingen presenterar två olika uppställningar av analoga modelleringsexperiment, termomekaniska- och centrifugexperiment. Dessa experiment simulerar lateral spridning av en jordskorpa bestående av tre lager, den undre-, mellan- och övre jordskorpan där mellanskorpan genomgår partiell smältning. I dessa modelleringsexperiment antas att spridningen är orsakad av skillnaderna i gravitativ potentiell energi mellan den förtjockade orogena jordskorpan och de tunnare angränsande områdena. Under experimenten har spridningen fritt utrymme. I centrifugmodelleringarna är spridningen gravitativ och förorsakar ett lateralt flöde som skapar domformade strukturer. I de termomekaniska modelleringarna är spridningen termisk och förorsakar endast lateralt flöde.

De analoga modelleringsresultaten visar att lateral och gravitativ spridning i en, på grund av ackretionstektonik, förtjockad jordskorpa med en duktil mellanskorpa förorsakar deformation i jordskorpans alla tre lager. Spridningen resulterar i tillplattning av den övre och den mellersta jordskorpan samt förtjockning av den undre och mellersta skorpan. Det sker även uttunning, förtjockning och extension av den mellersta och undre skorpan samt rotation av olika tektoniska block av jordskorpan.

Lateral spridningen kan även resultera i komprimering av lager och block samt överskjutningar, även om extensionsstrukturer dominerar. Spridningen roterar tektoniska gränser mot spridningsriktningen och tänjer ut skorpans olika lager. Uttänjning, förtunning, förtjockning och rotation av tektoniska

gränser är dominerande konsekvenser i den duktila mellanskorpan. De analoga modellerna visar att spridningen överskrider tektoniska gränser.

Geofysiska data - aeromagnetiska, seismiska reflektions- och refraktions-data - från den centrala delen av den Svekofenniska orogenesen har visat att det orogena bältet är sammansatt av olika fragment av jordskorpa, som är åtskilda av storskaliga skjuvzoner. De analoga modellerna antyder att storskaliga skjuvzoner i de seismiska profilerna är reaktiverade tektoniska gränser och ytor som tänjts ut och roterat västerut.

Geokronologiska, geokemiska och strukturella data från Paleoproterozoikum i Mellersta Finlands granitoidkomplex visar att plutonen har nått sin vertikala position under en post-ackretional period som förorsakat exhumering och lateral spridning av den mellersta jordskorpan. Exhumeringen och spridningen började vid ca. 1884 Ma och fortsatte ända till 1870 Ma. Bergarterna i den Mellersta Finlands granitoidkomplex kan delas in i tre grupper baserat på deras geokemi och åldrar. Bergarterna i Grupp 1 bildades genom partiell smältning av den nedre skorpan och magmorna kristalliserade >1887 Ma i den övre och mellersta jordskorpan. Bergarterna i Grupp 2 bildades genom partiell smältning av den mellersta jordskorpan och kristalliserade mellan 1890-1886 Ma i den övre skorpan (på sub-vulkanisk nivå) och ca 1884-1883 Ma i den övre delen av den mellersta skorpan. Magmorna som bildade bergarterna i Grupp 3 genererades genom exhumeringen av den nedre skorpan och de kristalliserade ca 1881-1880 Ma i de övre delarna av den mellersta skorpan. Varje grupp representerar en viktig händelse i jordskorpans evolution: Magmorna som bildade Grupp 1 är de första post-ackretionala smältorna av den förtjockade skorpan, magmorna som bildade Grupp 2 är resultatet av en omfattande uppsmältning av den mellersta skorpan förorsakats av radioaktivt sönderfall i de inre delarna av den förtjockade skorpan, och magmorna till Grupp 3 genererades genom extension. Jämförelsen mellan Mellersta Finlands granitoidkomplex och de angränsande områdena visar att likartade och samtida deformationer samt magmatism är närvarande i hela den centrala delen av den orogenin.

De analoga modellerna och data från den centrala delen av den Sveko-fenniska orogenesen i Finland antyder att den samtida exhumeringen och det laterala utflödet över hela orogenin kan förklaras av en gravitativ spridning västerut.

List of original articles

Paper I. Nikkilä, K., Roy Chowdhury, B.S., Dietl, C., Korja, A., Eklund, O., Zanella, F., 2009. Thermomechanical analogue modelling of the extensional collapse of a collisional orogeny, the Svecofennian orogen, Finland. Geotectonic Research 96, 21-38.

Paper II. Nikkilä, K., Korja, A., Koyi, H., Eklund, O., 2015. Analog modeling of one-way gravitational spreading of hot orogens – A case study from the Svecofennian orogen, Fennoscandian Shield. Precambrian Res. 268, 135-152.

Paper III. Nikkilä, K., Mänttäri, I., Nironen, M., Eklund, O., Korja, A., 2016. Three stages to form a large batholith after terrane accretion – An example from the Svecofennian orogen. Precambrian Res. 281, 618-638.

Contributions:

Paper I: Nikkilä is mostly responsible for the laboratory work excluding the CT- scanning. Nikkilä is fully responsible for the Figures 5-8, and 11. Nikkilä is mostly responsible for analog model interpretation, and first draft of experimental procedure and results. Roy Chowdhury is responsible for the Figures 3, 4, 9, 10 and 14, and she has drafted the manuscript. Dietl has supervised the laboratory work, and Korja and Eklund have participating in designing of the experiments. Korja is responsible for the Figures 1-2, 12-13 and drafting of the geological background, seismic profiles and their interpretation.

Paper II: Nikkilä is fully responsible for model preparation and illustration, and mostly responsible for laboratory work, model interpretation and drafting of the manuscript. Koyi has helped with the laboratory works. All co-authors have participated in designing of the experiments and drafting of the manuscript.

Paper III: Nikkilä is fully responsible for illustration of the Figures, except Figures 4 and 8. Nikkilä is mostly responsible for sample collection and selection, geochemical modeling, data interpretation and drafting of the manuscript. Mänttäri is mostly responsible for the zircon U-Pb age determinations and interpretations. All authors have participated in defining of the study area, designing and drafting of the manuscript.

Table of Contents

1 Introduction

The Paleoproterozoic Era (2.5–1.6 Ga) forms a unique period of the Earth's evolution. The continental crustal thickness increased and lithospheric plates became stronger at the Paleoproterozoic time (Rey and Coltice, 2008), changing the continental plate configuration and tectonic processes compared to the Archean (e.g. Corrigan et al., 2009). An important event during the Paleoproterozoic era has been the assembly of the proposed supercontinent Nuna, during which Paleoproterozoic orogens formed (Zhao et al., 2004). The orogens are characterized by long, linear mobile belts such as the Trans-Hudson (Cawood et al., 2009; Corrigan et al., 2009) and the Svecofennian orogens (Lahtinen et al., 2005).

Accretionary and collisional orogens have been important in terms of the production and preservation of juvenile continental crust during the Paleoproterozoic (Cawood et al., 2006; 2009; Condie, 2014). In an accretional orogeny, arc components are juxtaposed together and/or with continental margins (Cawood et al., 2009). The arc materials can have different compositions prior to juxtaposing leading to orogenic crust with mechanical heterogeneity in crustal components (Fig. 1; e.g. Mooney et al., 1998; Jagoutz and Schmidt, 2012; Jamieson and Beaumont, 2013). The accretionary orogens are evolved into collisional orogens when the ocean closes (Cawood et al., 2009). Collision leads to modification of the accreted, continental crust and production of post-accretion granitic batholiths, for example, in the Himalayan or Variscan orogenic belts (Condie, 1973; Paterson and Miller, 1998; Vanderhaeghe et al., 1999; Cawood et al., 2009; Vanderhaeghe, 2009; Jagoutz and Schmidt, 2012).

Accretion or collision can take place by thick or thin-skin (thicker and thinner lithological pieces, respectively) stacking (Fig. 1; Goleby et al., 1989; Coward, 1996; Culshaw et al., 2006; Nemčok et al., 2013), whereupon tectonic boundaries are present in the orogen. New structures may arise from mechanical boundaries between and within the converging crustal blocks, and the structures may be reactivated several times after deformation events (e.g. Burg and Ford, 1997; Fossen and Rykkelid, 1992; Holdsworth et al., 1997; Jackson, 1980).

Orogenesis leads to thickening of the crust, and crustal thickening can lead to thermal relaxation (Huerta et al., 1996). Thermal relaxation results from radioactive decay mainly by U, Th and K, which generates heat within the crust (England and Thompson, 1986). The thermal relaxation can lead to partial melting of the constituting rocks. The partial melts can be accommodated deeper in the crust forming magma batches or magmas can be transported upwards (Vigneresse, 1995; Petford et al., 2000; Vanderhaeghe and Teyssier, 2001). If there are enough partial melts in the crust (>7 %;

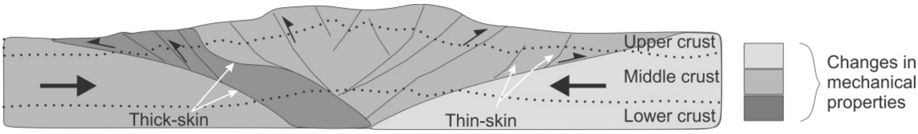

Figure 1. Schematic model of a thickened crust. In an accretionary orogen different crustal components with mechanical heterogeneity can be found. Thick- and thin-skin stacking surfaces form weakness zones with a three-layer crust. Figure modified after Nemčok et al. (2013).

Brown, 2007) a low-viscousity layer can be formed (Vanderhaeghe and Teyssier, 2001).

Partial melting allows magma segregation and transportation (Vigneresse, 1995), which lead to crustal differentiation and a heterogeneously stratified three-layer crust (Fig. 1; Mooney et al., 1998; Mooney 2015 and references therein). Seismic P-wave velocities suggest that granitic and metasedimentary rocks are predominate in the upper crust, intermediate plutonic rocks and amphibolite-grade metamorphic rocks in the middle crust (Mooney 2015 and references therein), and gabbroic plutonic rocks and granulites in the lower crust (Vanderhaeghe, 2009 and references therein). The crustal differentiation can be related to the orogenic processes, but a three-layer crust may also develop into thick, mature island arcs and into thick oceanic plateaux prior to accretion (Mooney et al., 1998; Tetreault and Buiter, 2014).

If the thickened crust has excess in gravitational potential energy (GPE) compared to its thinner surroundings, then the material may spread outward causing thinning of the orogenic core and thickening of the surrounding areas (Rey et al., 2001; Vanderhaeghe and Teyssier, 2001). The outward spreading takes place in the upper crust or in the middle and lower crusts (Vanderhaeghe et al., 1999; Rey et al., 2001), where partial melting decreases viscosity enabling large-scale horizontal flow (Beaumont et al., 2004; Royden, 1996; Willett, 1999). Such gravitationally induced spreading of the thickened crust is usually called gravitational collapse (Rey et al., 2001; Vanderhaeghe and Teyssier, 2001), orogenic collapse (Teng, 1996; Lahtinen et al., 2005), or gravitational spreading (e.g. Jamieson and Beaumont, 2011; Paper II). Hereafter, the term gravitational spreading is used in order to stress the GPE differences as the causing force and spreading as the main result.

The presence of inherited structures and crustal layering can affect to the development and the style of late orogenic deformation. Variations in the boundary conditions, such as free- or fixed flanks, may also lead to different development of deformation in late orogenic spreading or collapse (Rey et al., 2001; Cagnard et al., 2006; Harris et al., 2012). Several studies on reactivation of large-scale structures during post-collisional deformation emphasize the significance of pre-existing structures (Fossen and Rykkelid, 1992; Frisch et al., 2000; Ranalli, 2000; Ziegler et al., 1998). However, the role of crustal-scale structural inheritance in post-accretion gravitational spreading, and how the mechanical strength variations steer the process, are only vaguely known.

To distinguish the new structures from the inherited ones is difficult, and therefore different tectonic alternatives have been considered for the interpreted structural geometries by geodynamic models (e.g. Corti et al., 2001; Jamieson et al., 2010; Tetreault and Buiter, 2012; Paper II). Although the geodynamic models help to understand the prevailing post-accretion processes, the models need to be compared with information gained from geological and geophysical studies. However, the geological studies give information mainly from the surface. When deciphering crustal structure or creating tectonic models, seismic data are crucial for definition and comparison of deeper structures (e.g. INDEPTH: Nelson et al., 1996; Brown et al., 1996; Meissner et al., 2004; Culshaw et al., 2006. LITHOPROBE: Corrigan, 2012; FIRE: Sorjonen-Ward, 2006; Korja and Heikkinen, 2008; Kukkonen et al., 2008; Papers I and II).

Characterization of ancient deeply eroded orogens is important in order to understand modern orogenic processes. In this thesis, the Paleoproterozoic Svecofennian orogen in the Fennoscandian Shield is used as an example of an ancient accretionary orogen that has undergone post-accretion magmatism and deformation. For the reconstruction of post-accretionary extensional events, combined geological and geophysical data from the central part of this orogen are compared to geodynamic, analog models.

The evolution of the central part of the Svecofennian orogen has been discussed and re-interpreted during the last decade (Fig. 2; e.g. Lahtinen et al., 2005, 2009; Korja et al., 2006), and it is a general agreement that a Paleoproterozoic arc or microcontinent accreted against the Archean crust ca. 1.91 Ga. However, the post-accretion/-collisional events have been under debate: A gravitational spreading at

1.88-1.87 Ga or 1.87-1.86 Ga (Lahtinen et al., 2005; Korja et al., 2006, 2009; Paper I, II, III), a post-magmatic crustal scale imbrication (maybe at 1.84-1.80 Ga; Sorjonen-Ward, 2006), a buckled Bothnian orocline at 1.87-1.86 Ga (Lahtinen et al., 2014), and a lower crustal delamination at 1.85 Ga (Kukkonen et al., 2008) have been suggested. In addition, there are variations in the interpretation of formation of large-scale structures, such as the crustal scale high reflective areas in the seismic data (FIRE; Sorjonen-Ward, 2006; Kukkonen et al., 2008; Korja et al., 2009). In all these interpretations three-layer crust has been defined (Korja et al., 2006; Korja and Heikkinen, 2008; Korja et al., 2009; Lahtinen et al., 2009; Sorjonen-Ward, 2006; Kukkonen et al., 2008).

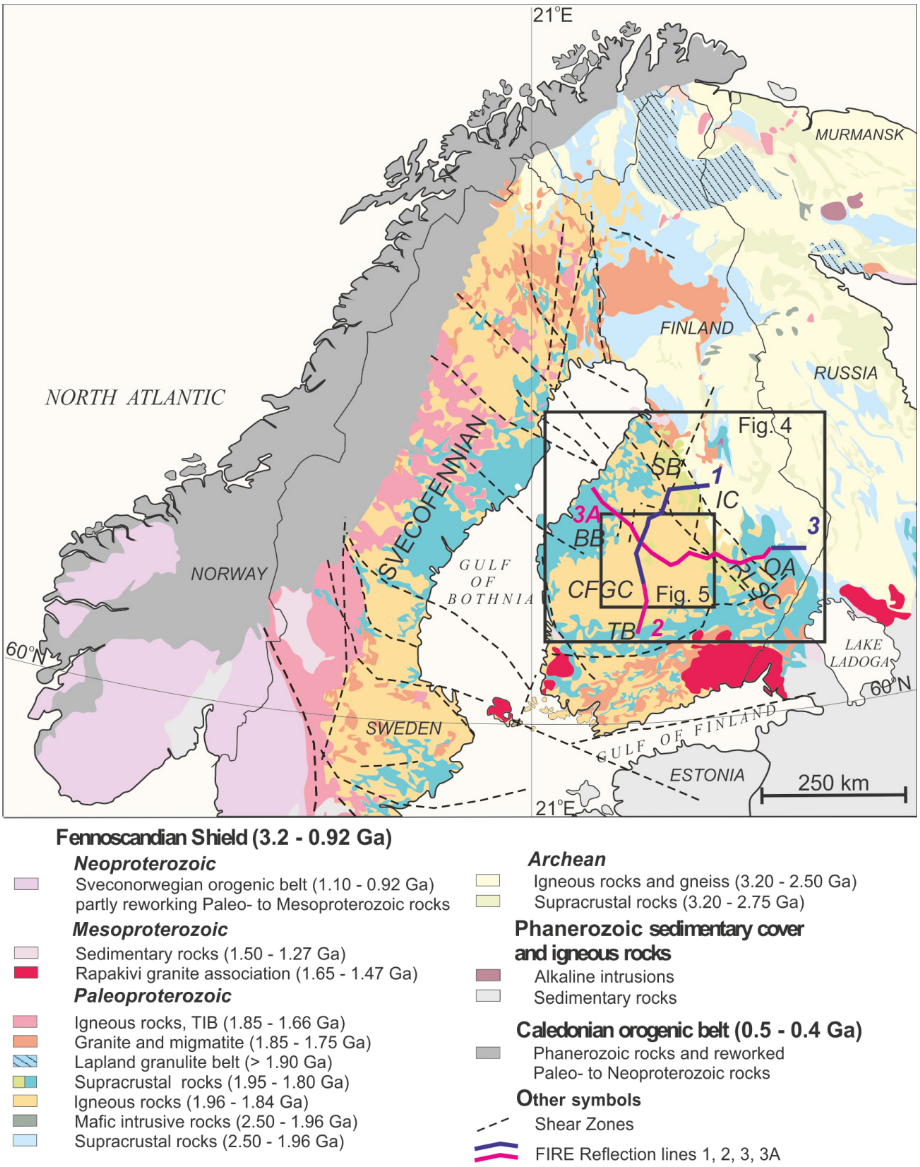

Figure 2. The main lithological units of Fennoscandia (Koistinen et al., 2001; Lahtinen et al., 2005) and seismic profiles (Kukkonen et al., 2006). *Abbreviations: BB – Bothnian Belt; CFGC – Central Finland granitoid complex; IC – Iisalmi complex; OA – Outokumpu area; RLSC – Raahe-Ladoga shear complex; SB – Savo belt; TB – Tampere belt.*

1.1 Objectives of the study

This work has been aiming to understand Paleoproterozoic crustal evolution and its dynamics, especially the post-accretionary features of the Svecofennian orogeny (Fig. 2). The thesis presents and discusses the contribution of analog models of extensional collapse and gravitational spreading (Papers I and II) to geophysical and geological data from the core of the Paleoproterozoic orogen (Papers I, II and III).

The main questions have been how a thick three-layer crust with a thick (> 20 km) partially molten layer is deformed under lateral and/or gravitational spreading, and whether there is evidence of such deformation in the central part of the Svecofennian orogen in Finland. The research questions of this thesis are the following:

1) How will an over-thickened three-layer crust, with weak middle crust, deform at post-collisional stage during lateral spreading?
2) How do tectonic boundaries reactivate and deform during gravitational spreading?
3) How does an orogen with lateral mechanical heterogeneity deform during gravitational spreading?
4) What have been the duration, timing and mechanism of the post-accretion event/deformation in the Paleoproterozoic crust in the central part of the Svecofennian orogen?
5) Did the central part of the Paleoproterozoic Svecofennian orogen undergo gravitational spreading?

The relationship between the research questions and Papers are illustrated in Figure 3.

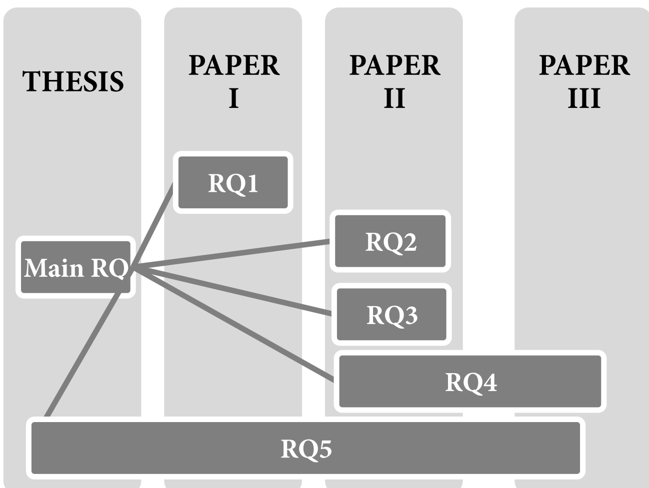

Figure 3. The relationship between the Research questions (RQ), Papers and thesis.

2 Geological background of the studied area

2.1 The Svecofennian accretionary orogen in Central Finland

The Paleoproterozoic Svecofennian orogen is located in the central part of the Fennoscandian Shield. The accretionary stage in central Finland occurred at 1.91-1.88 Ga, when Paleoproterozoic terranes accreted against the Archean continental margin (Fig. 2; Lahtinen et al., 2005; Korja et al., 2006). The central part of the orogen is composed of Archean and Paleoproterozoic rocks in the east and west, respectively. The terrane accretion, magmatism and collision thickened the crust up to ca. 72 km (Väisänen et al., 2002; Paper II).

The Svecofennian orogen hosts an exhumed low pressure - high temperature metamorphic orogenic core (Korsman et al., 1999a) typical for large hot orogens (Collins, 2002; Chardon et al., 2009). The exposed crustal level represents a section through the lower part of the upper crust and the upper parts of the middle crust (Sorjonen-Ward, 2006; Kukkonen et al., 2008; Korja et al., 2009).

Based on lithology, geochronology and metamorphic grade, the rock units have been divided into several complexes separated by faults or ductile deformation zones by Nironen et al., 2002 (Fig. 4A). The complexes in the central part of the orogen are the following: the Archean Iisalmi complex (IC), the Paleoproterozoic Outokumpu area (OA), the Savo belt (SB), the Bothnian belt (BB) and the Central Finland granitoid complex (CFGC) (Fig. 4A). The large-scale Raahe-Ladoga shear complex is transecting the suture area of the Iisalmi complex, the Savo belt and the Outokumpu area (Korsman et al., 1999b).

The IC (3.2–2.6 Ga) is composed of tonalitic gneisses and amphibolitic migmatites (e.g. Ruotoistenmäki et al., 2001; Halla, 2005; Hölttä et al., 2012), and has been intruded by granitic and gabbroic plutons at ca. 1.88-1.86 Ga (Fig. 4B; e.g. Ruotoistenmäki et al., 2001). The metamorphic grade increases westward from upper amphibolite to upper granulite facies (Hölttä and Paavola, 2000; Hölttä et al., 2012). The main rock types in the OA (1.97 Ga; Huhma 1986) are schist, gneisses and migmatitic gneisses (Sorjonen-Ward and Luukkonen, 2005). Also in the OA, the metamorphic grade increases westwards from low-P amphibolite facies to low-P granulite facies (Kontinen et al., 1992, Sorjonen-Ward, 2006). The SB (1.9 Ga) is an arc complex, composed of metavolcanic and metasedimentary rocks (Lahtinen and Huhma, 1997; Kähkönen, 2005), metamorphosed in low-P – medium-T amphibolite facies (Hölttä, 1988; Korsman et al., 1999). In the BB (1.8–1.9 Ga) the middle crustal units are exposed in a domal structure (Korja et al., 2009; Hölttä, 2013). The metamorphic grade increases from mid-amphibolite to granulite facies toward the core of the complex (Hölttä, 2013). The CFGC,

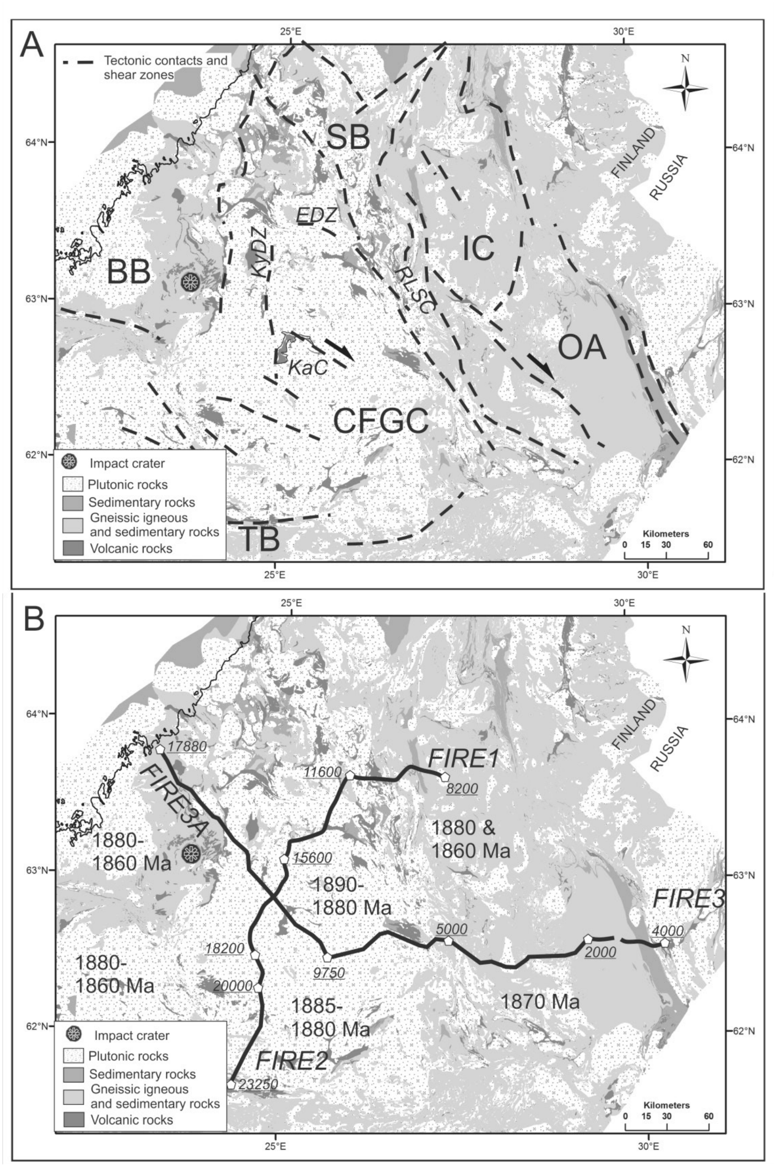

Figure 4. A simplified lithological map of the central part of the Svecofennian orogen (modified after Korsman et al., 1997; Paper II). The location of the map is shown in Fig. 2. A) The tectonic contacts and the major shear zones (after Papers II & III), and lithological-geographical areas of the orogenic belt (after Nironen et al., 2002). *Abbreviations: Archean units: IC – Iisalmi complex; Paleoproterozoic units: BB – Bothnian belt; CFGC – Central Finland granitoid complex; EDZ – Elämäjärvi detachment zone; KaC – Kalmari subvolcanic complex; KyDZ – Kyyjärvi deformation zone; OA – Outokumpu Area; RLSC – Raahe-Ladoga shear complex; SB – Savo belt; TB– Tampere Belt.* B) The emplacement ages of post-accretional plutonic rocks (the range is based on U-Pb ages from FinnAge database). And the seismic profiles, which are used in this thesis. Underlined numbers denote CMP locations on FIRE1, 2, 3 and 3a.

a large granitic batholith, is located in the west-central part of the orogen. The CFGC is limited by the Raahe–Ladoga shear complex in the east, the low-angle Elämäjärvi detachment zone to the north, subvertical shear zone at the boundary to the west and Tampere belt in the south (Fig. 4).

The CFGC has been emplaced during post-collisional orogenic events at 1.89-1.87 Ga (Fig. 4B; Nironen, 2003; Rämö et al., 2001). The batholith comprises mainly felsic to intermediate plutonic rocks from tonalite to granite, where granodiorite is most common rock type. Mafic plutons are rare and they are represented by small gabbroic to quartz dioritic intrusions that are mainly related to shear zones and coeval with the emplacement of the youngest CFGC granites (Nironen et al., 2000; Rämö et al., 2001). Minor amounts of predominantly felsic to intermediate volcanic to subvolcanic rocks are also present together with minor mafic volcanic rocks and rare metapelitic rocks (Nironen, 2003; Vaarma and Pipping, 2003). The subvolcanic to volcanic rocks (ca. 1887±2 Ma; Nironen, 2003; Paper III) are mainly found in the Kalmari complex in the middle part of the CFGC (Fig 5; Rämö et al., 2001; Nironen, 2003).

The CFGC was chosen for a study area due to its central location in the Svecofennian orogen, and due to the interpretations of the gravitational and lateral spreading in the area (e.g. Lahtinen et al., 2005; Korja et al., 2006; 2009). Furthermore, the detailed study area with sample locations was chosen due to its central location in the CFGC, the intersection of the seismic profiles (FIRE1 and 3a), and the expectance to find representative assemblage of the rocks and the deformation types in the CFGC.

2.2 The crustal structure of the Svecofennian orogen

In the central part of the Svecofennian orogen, the crust is up to 65 km thick at present (Grad and Tiira, 2009). Seismic refraction data suggest a felsic upper, an intermediate middle and a mafic lower crust (Grad and Luosto, 1994; Kuusisto et al., 2006). Korja et al. (2009) proposed that the middle crust has had enough partial melts at the post-collisional stage, similarly to Tibetan plateau today (Nelson et al., 1996), allowing lateral spreading.

The seismic reflection profiles FIRE1&3a (Finnish Reflection Experiments) transects the central part of the Svecofennian orogen and they images a frozen picture of the three-layer crust (Fig. 6A; Kukkonen et al., 2006). The layer boundaries are highly reflective zones (Korsman et al., 1999a; Korja et al., 2009), and interpretations of tomographic Vp/Vs ratio models indicate lateral changes in elastic properties across the orogen (Hyvönen et al., 2007). Korja (1993), Hjelt et al. (2006) and Korja and Heikkinen (2008) proposed that the crustal scale conductors and changes in the reflection patterns mark terrane boundaries within the orogen.

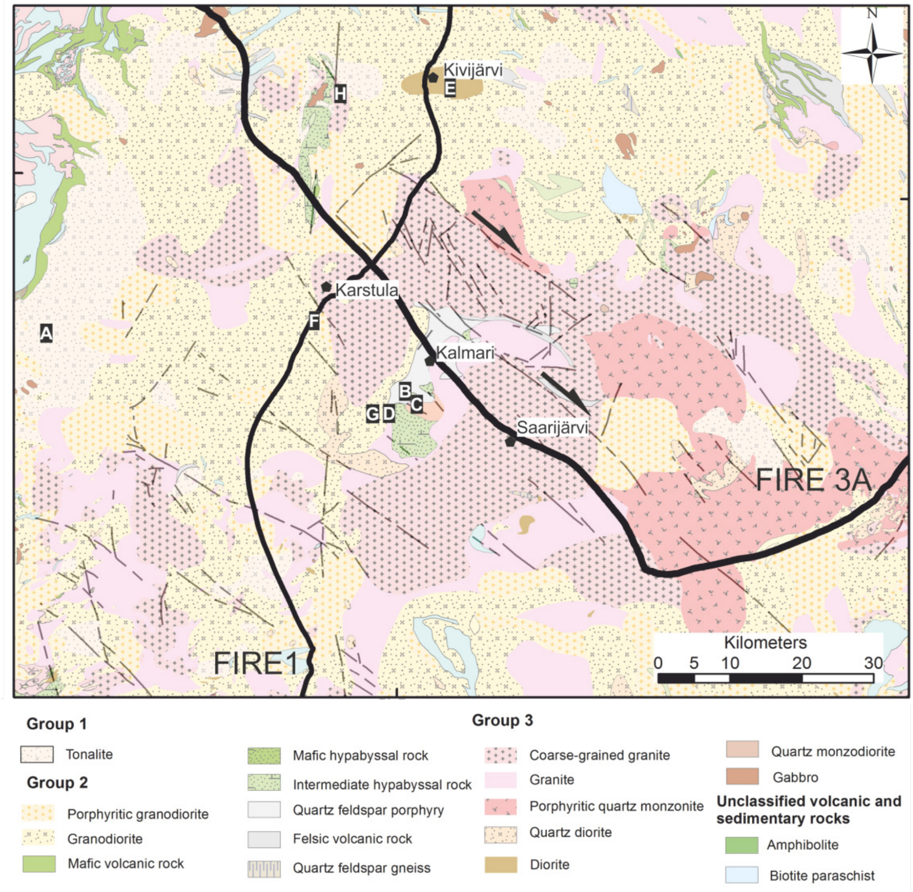

Figure 5. A lithological map showing the distribution of the Group 1-3 igneous rocks and the location of SE-NW trending shear zones in the central part of the CFGC (Paper III). See Fig. 2 for location. The letters with black background indicate the locations of the U-Pb zircon ages (Paper III): A– ≥1887 ± 3 Ma; B– 1890 ± 4 Ma; C– 1887 ± 2 Ma; D – 1886 ± 3 Ma; E– 1881 ± 2 Ma; F – 1884 ± 2 Ma; G – 1883 ± 3 Ma; H – 1880 ± 2 Ma.

2.3 Distributed deformation

In the CFGC, the degree of deformation varies from undeformed, to gneissic, spaced or penetrative foliation, and to localized mylonitic deformation (e.g. Nironen et al., 2000; Nironen, 2003; Vaarma and Pipping, 2003; Paper III). In general, the penetrative foliation is interpreted to have formed during contraction processes (Nironen et al., 2000; Nironen, 2003), but some mylonitic deformation is related to younger transtensional shearing (Nironen, 2003; Kilpeläinen et al., 2008).

The gneissic foliation is found in granodiorites (Nironen et al., 2000) and tonalites (Lahtinen, 1994). The low-angle, E-W trending, mylonitic shear zone (Elämäjärvi) with penetrative stretching lineation represents ductile deformation and indicates westward movements in the northern part of the CFGC (Kilpeläinen et al., 2008). The subvertical localized shear zones are NW-SE trending in the CFGC and occur in granites. They have a horizontal dextral kinematic component (Nironen et al., 2000) and moderate SE-plunging lineation (Korja et al., 2009) suggesting an oblique slip shear zone with south-side uplift (Paper III). This is in agreement with the results from Selonen and Ehlers (1996) that also indicate a southwest-side up movements of a granitic pluton in the southern part of the CFGC.

3 Methods

3.1 Thermomechanical analog models

Thermomechanical analog modeling was adapted to simulate extensional collapse (Paper I). The experiments were made at the Johann Wolfgang Goethe University in the Frankfurt, Germany. The apparatus consisted of a basal PVC plate, which could be heated, and of four walls: two fixed and two adjustable to be moved at moderate to low rate. One of the adjustable walls was tensional and moved at higher rate compared to the compressional one.

The models had three layers, which represented upper, middle and lower crusts. The layers were made out of plasticine and sand. The plasticine was mixed with pharmaceutical white oil (liquid paraffin) in order to make it less viscous. To create ductile, low-viscous middle layer, more oil was added than to the lower layer.

The modeling procedure and materials used in this study are described in Paper I. More detailed information of the modeling apparatus is found in Roy Chowdhury et al. (2009).

3.2 Centrifuge analog models

Centrifuge analog modeling was adapted to simulate gravitational spreading (Paper II). The experiments were made with a large centrifuge in the Hans Ramberg Tectonic Laboratory at Uppsala University. In this modeling, the centrifugal force field simulated the Earth's gravitational field. Due to the vertical position in the centrifuge, the real gravitation field caused the tectonic movements within the model. The model was placed in to a Perspex box, with three fixed walls and one wall that could be moved. Hence, the extension was unilateral.

The models consisted of two blocks and three layers, representing upper, middle and lower crusts. All modeling materials were based on pure plastilina® (modeling clay) into which oil, sugar powder, silicone and/or barium sulfate were mixed in order to reduce or increase density and/or viscosity. The composition of the individual layer materials were chosen to reflect temperature effect on rheological properties in such way that the weakest layer was in the middle.

Modeling procedure and description of the used material properties are presented in more detailed in Paper II. More information of the large centrifuge apparatus is found in Harris and Koyi, 2003.

3.3 Geochemical analysis

For major and trace – including rare earth elements (REE) – compositions, 57 samples were analyzed from the Central Finland granitoid complex (Paper III). In addition, 151 geochemical analyses were selected from the GTK Litogeochemical database (Rasilainen et al., 2007). The analyses were done by the Labtium Oy laboratory and all samples were analyzed with the same methods. The accepted methods are certified (codes are 175X, 308, 308M and 725I) and described by Rasilainen et al. (2007).

3.4 Zircon U-Pb analysis

Eight samples were collected for zircon U–Pb dating to constrain the temporal variation of the igneous rocks in the CFGC (Paper III). The U–Pb isotope analyses were made using the Nordic Cameca IMS 1280 at the NordSIMS laboratory at Swedish Museum of Natural History, Stockholm, Sweden. The zircons were selected by hand-picking after heavy liquid and magnetic separation. The data calculations and presentations were done using the Isoplot/Ex 3 program (Ludwig, 2003).

The more detailed description of the samples and used programs are found in Paper III. For detailed analytical procedure see Whitehouse et al. (1999) and Whitehouse and Kamber (2005).

4 Summaries of the original papers

4.1 Paper I: Thermomechanical analogue modeling of the extensional collapse of a collisional orogeny – the Svecofennian orogen, Finland

Paper I represented a set of thermomechanical analog models of extensional collapse of a collisional orogen (Fig. 6B). The aim of the experiments was to study the development of large-scale structures and the deformation of a thick (80 km), three-layer crust during an extensional collapse and crustal flow. In the models, the weakest layer was in the middle to represent widespread partial melting of the thickened orogenic crust.

The model properties of pure plasticine (lower layer), plasticine with oil (middle layer) and sand (brittle upper layer) were used. The models were extended and compressed simultaneously to produce a "collapse" environment. The apparatus consisted of a heated plate, which increased the temperature and thus reduced the viscosity of the model before and during the experiments. The middle and lower layers of the models deformed by viscous flow, while the upper layer deformed by brittle faulting. The deformation of the models started by flow in the middle layer and continued upwards; hence the middle layer was flowing before the upper layer deformation.

The experiments showed that the deformation was unevenly distributed between the model layers (Fig. 6B). In models both normal and reverse faults developed in the upper and middle layers, but only normal ones formed in the lower layer. The faults and the shear zones continued across the upper- middle layer boundary, but not across the middle-lower layer boundary. In models, a large shear zone (transpressive) transecting the upper- middle layer boundary developed and, once it was formed, all the deformation was concentrated on it. The upper layer formed graben and horst structures. The middle layer thinned below the transpressive shear zone and thickened further away from the shear zone. The lower layer thickened below the transpressive shear zone and thinned in those places, where the middle layer had thickened.

The experiments show that small changes in the viscosity do not change the style of the large-scale structures (i.e. lower crust sunk down; weakness zones across upper-middle layers, thinning and subsidence).

The thermomechanical analog modeling results were compared to the central Svecofennian orogen using images along the deep seismic reflection profiles FIRE1 and 3a. Thinning of lower and middle layers, faulting in the brittle upper and the highly viscous lower layers, and the subsidence of upper and middle layers, were similar to interpretations of the FIRE1 and 3a profiles (Fig. 6B). The results in Paper I show that the extension of the collapse can start from bottom, i.e. the lower crust, and advance upwards forming normal

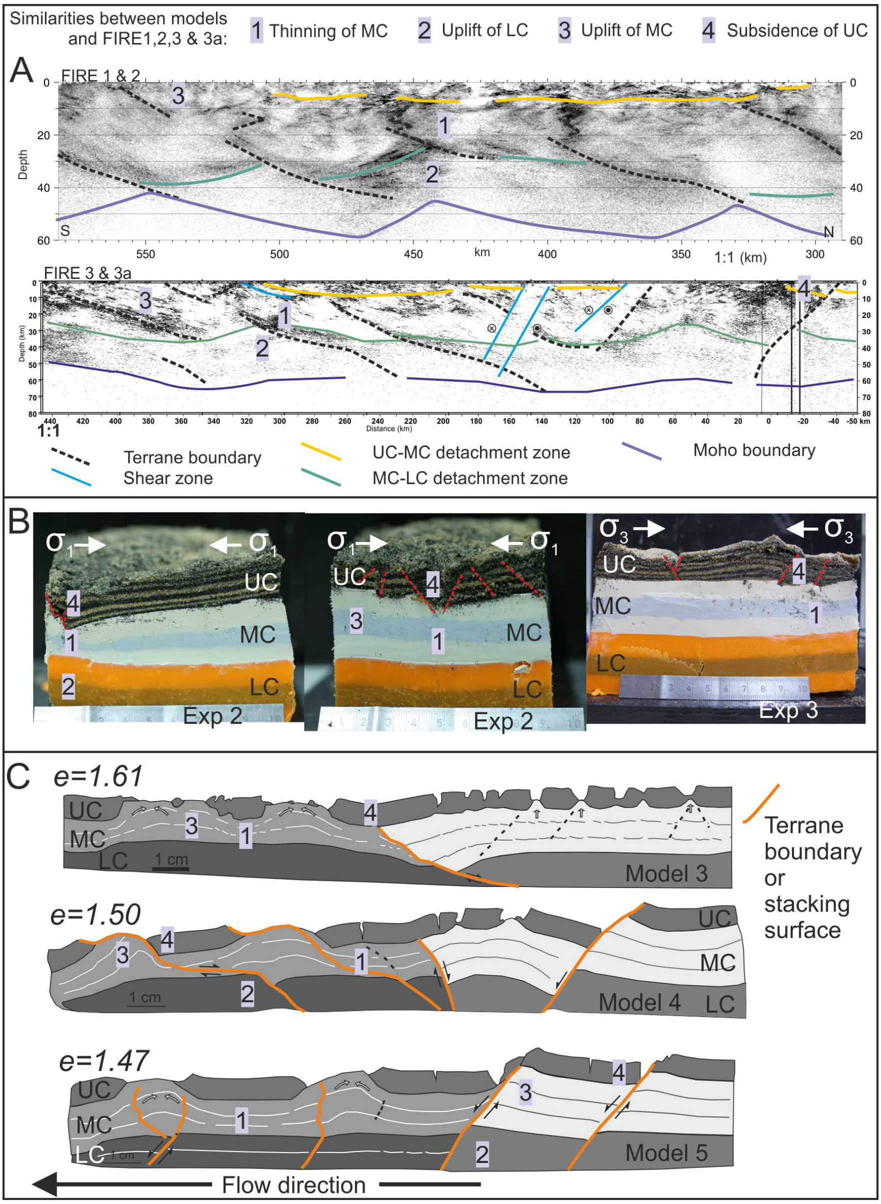

Figure 6. A comparison of the crustal structures in the FIRE1, 2, 3 & 3a reflection profiles and the analog models from Papers I and II. The numbers 1-4 denote similarities between the FIRE profiles and the analog models. A) An interpretation of FIRE 1-3 profiles. Upper panel: FIRE 1 &2 simplified from Paper III. Lower panel: FIRE 3 & 3a simplified from Papers I and II. B) The results from thermomechanical analog experiments 2 and 3 (Paper I). The experiments show normal and reverse faults in the upper layer in both extension and compression directions, and ductile thinning of the middle layer. C) Results from the centrifuge analog modeling (models 3-5; Paper II). The models show terrane boundary elongation (models 3 and 5) and shortening (model 4), elongation and rotation of the stacking surfaces (models 4 and 5). The amount of extension is indicated with elongation (e). Abbreviations: *UC – Upper crust/layer; MC – Middle crust/layer; LC – Lower crust/layer.*

faults and horst-graben structures in the upper crustal layers. In Paper I, it was also concluded that the flowing of the middle and lower crusts during extensional collapse can produce features similar to those imaged in deep seismic reflection profiles of the Svecofennian orogen.

4.2 Paper II: Analog modeling of one-way gravitational spreading of hot orogens – A case study from the Svecofennian orogen, Fennoscandian Shield

Paper II studied one-way gravitational spreading (collapse) of an accreted orogen with a three-layer thick crust by analog centrifuge experiments (Fig. 6C). The aim of the study was to test the effect of inherited crustal components (terranes and pre-existing weakness zones), and tectonic boundaries on crustal-scale lateral flow of a gravitationally unstable crust. In the experiments, it was assumed that the compressional stage of the orogeny had stopped to distinguish the deformation events, resulting from the gravitational spreading, from the collisional ones.

The experiments were divided into two series. The first series tested, how a thickened crust deformed in the presence of two mechanically contrasting crustal blocks and how the mutual block boundary behaved during gravitational spreading. The second series tested the effect of additional inherited tectonic boundaries, such as stacking surfaces or strike-slip faults, during gravitational spreading. In all the experiments, the extension was unilateral and the mechanically weakest layer was placed in the middle.

The results gave insights into the role of inherited crustal scale weakness zones during post-collisional gravitational spreading. The deformation was heterogeneous across the models and was guided by the tectonic boundaries and the mechanically different blocks. The number of weakness zones, the dip direction of the weakness zones related to the flow direction and the mechanical properties affected the deformation patterns both in crustal and regional scale. The deformation took place via 1) tilting and rotation of the weakness zones and the subblocks, 2) elongation and shortening of the crustal layers, the subblocks and the weakness zones, 3) thinning and thickening of the crustal layers and the subblocks, and 4) by normal faulting in all the crustal layers.

The deformation was concentrated into the pre-existing weakness zones. In models where only one block boundary was present, the boundary accommodated more deformation (e.g. elongation of the boundary was up to 90 %) compared to the blocks A and P. In models with many pre-existing weakness zones, the deformation was distributed evenly across the zones.

The unilateral extension rotated/tilted the pre-existing weakness zones towards the extension direction and caused doming. In the models without pre-existing weakness zones the doming was symmetric within the blocks, and with pre-existing weakness zones, the doming was asymmetric. The results indicated that the deformation signature in the accreted orogens might be variable and that large-scale shortening (Fig. 6C; e = 1.50), extension and rigid block and fault rotation might occur simultaneous with gravitational spreading. The modeling suggested a 16-23 my duration for gravitational spreading of ca. 50 %. The more pre-existing weakness zones there were, the shorter was the duration of the spreading.

The centrifuge analog modeling results were compared to the deep seismic reflection profiles FIRE1 and FIRE3, refraction profile BALTIC, and to the lithology of the central part of the Svecofennian orogen in Finland. The modeling results and the seismic profiles have similar change in the crustal layer thicknesses. The bright reflective bands, both the low-angle listric and the zigzag shape in the FIRE profiles, can be explained by either reactivation of terrane boundaries or by thick-skin stacking surfaces.

The changes in the metamorphic grade in the OA, in the IC and in the BB, can be explained by crustal scale block rotation and by large scale doming. The modeling also indicates that the post-accretion gravitational spreading may not have thinned the crust more than 20%. This may explain the thick crust not only in the Fennoscandian Shield, but also in other low topography Paleoproterozoic Shields elsewhere.

4.3 Paper III: Three stages to form a large batholith after terrane accretion – an example from the Svecofennian orogen

Paper III studied geochronological and geochemical interpretations of a batholith formed in an accretionary orogen. The aim of this paper was to investigate the relationship between the deformation, the timing of events by the geochronology and the geochemistry of plutons, and to more precisely define the timing of deformation in the central part of the Svecofennian orogen (Table 1).

The results show that by using the combination of U-Pb zircon ages and the geochemical signature of the plutons constituting the CFGC batholith, they can be divided into three groups, which correspond to a specific stage of the post-accretion events. Calcic tonalites belong to Group 1 (≥1887 ± 3 Ma), and they represent partial melts of the lower crust that has generated normal arc type magmas. Calc-alkalic plutons and (sub)volcanic rocks belong to Group 2. The (sub)volcanic rocks and the granodiorites, 1890-1886 Ma and 1884-1883 Ma, represent partial melts of the middle crust that generated normal arc type magmas. Calc-alkalic, alkali-calcic and alkalic gabbros,

Table 1. A compilation of lithological, geochemical, age and deformation data of the igneous Groups 1-3 in the CFGC (Paper III).

	Rock type	calcic	calc-alkalic	alkali-calcic	alkalic	Deformation: Pervasive	Deformation: Local	Undeformed	Age (Paper III)
Group 1	Tonalite	x				x		x	≥1887 ± 3 Ma
Group 2	Felsic volcanic rock		x			x	x	x	1886±3 - 1887±2 Ma
	Felsic subvolcanic rock			x			x	x	1890±4 Ma
	Granodiorite		x			x		x	1883±3 and 1884±2 Ma
Group 3	Diorite, Gabbro		x			x		x	1881±2 Ma
	Granite		x	x	x	x	x	x	1880±2 Ma
	Monzonite, Quartz-monzonite and -syenite			x	x		x	x	

diorites, granites, quartz-monzonites and quartz-syenites belong to Group 3 (1881-1880 Ma), and that result from the partial melting of the lower crust.

The interpretation suggests that the Group 1 magmas represent the first melts after accretion, the Group 2 magmas represent the main melting event, and the Group 3 rocks represent the melts that have formed and have been transported during lateral spreading, i.e. during an extensional event. The formation and the emplacement of the plutons of the Group 2 has lasted from ca. 1890 Ma to ca. 1883 Ma and has overlapped with the formation and the emplacement of the Group 1 plutons. The main melting event weakened the middle crust and enabled lateral flow. The Group 3 partial melts were transported to their emplacement level that was in ductile to semi-ductile environments at 1881-1880 Ma. The Group 3 magmas emplaced within a short time span, facilitated by the presence of crustal scale pre-existing shear zones (Fig. 6A).

The degree of deformation is not correlated with the emplacement ages as previously proposed (e.g. Nironen et al., 2000). The new age results show that the lateral flow, which caused the deformation, was active after the emplacement of the granodiorite at ca. 1884 Ma, still active during the emplacement of the Group 3 rocks at ca. 1881-1880 Ma and a short period thereafter. In the CFGC, the youngest low-angle deformation occurred between 1870-1860 Ma (Kilpeläinen et al., 2008), hence a duration of ca. 10-25 my for subhorizontal spreading in the CFGC is suggested.

5 Discussion

5.1 Simplifications of analog models

Geodynamic models are always simplifications of natural analogs. The models are not intended to be detailed simulations of natural processes, but to give insights on how these can be interpreted. To produce realistic geodynamic models some assumptions equivalent to nature need to be made. The models, produced in this thesis, are based on the presence of thickened unstable crustal architecture found in modern orogens (e.g. Nelson et al., 1996; Beaumont et al., 2004; Royden et al., 2008), and on seismic studies of crustal structure in the central part of the Svecofennian orogen in Finland (e.g. Korja et al., 1993; Luosto and Heikkinen, 2001; Kukkonen et al., 2006; Kuusisto et al., 2006).

Paper II tested deformation of terrane boundaries and thick-skin stacking surfaces during gravitational spreading. These surfaces are modeled as continuous structures from the upper or the middle layer continuing to the bottom of the analog models (Paper II). In the accretionary orogens, the stacking surfaces and the terrane boundaries can be e.g. continuous, attached to the layer boundaries or continuing within one crustal layer only (Molnar and Tapponnier, 1977; L´emos et al., 1992; Meissner et al., 2004; Culshaw et al., 2006). In addition, the amount of gentle-dipping structures increases with crustal depth (Culshaw et al., 2006). However, the terrane boundaries are reactivated often as a major strike-slip zone, especially in oblique collision zones (like the accretionary Svecofennian orogen in the central Finland; Lahtinen et al., 2005), resulting in major steeply dipping structures parallel to the orogenic belt (Molnar and Tapponnier, 1977; Scheuber and Gonzalez, 1999). Furthermore, during the terrane accretion, compression will develop steep reverse faults or rotate pre-existing surfaces and faults steeper. In the analog models (Paper II), the moderately to steeply dipping structures were used to simulate the deformation of the strike-slip shear zones, and to test how the steeply dipping surfaces resist the layer flow during gravitational spreading.

The effect of erosion, deposition of new sediments and other orographic processes have not taken account in the experiments (Papers I and II), even though it is assumed that they have been active both during and after the orogeny (e.g. Willett, 1999). Vanderhaeghe et al. (1999) and Beaumont et al. (2001; 2004) have proposed that surface processes have enhance extrusion of the middle/lower crustal material to shallower levels during gravitational spreading. However, in geodynamic models the rate and the amount of sedimentation and erosion are usually tested to find the best solution (Willett, 1999; Beaumont et al., 1999; Jamieson and Beaumont, 2013). The focus of this study has been on the deformation at deep levels of the crust and the interpretations of an exhumed crust of an ancient orogen with a 10-15 km deep crustal section (Papers I and II). Therefore the uppermost parts of the models have been removed, and the effect of erosion and deposition on the results is minimal. In addition, because the exposed section is below the former brittle-ductile transition zone, the role of the zone has not been considered in the interpretations of the models.

5.1.1 Post-collisional/-accretional weakening

The models were built to represent a stage after the main shortening, thickening, and thermal relaxation of an orogen (Papers I and II). The results are compared to the central part of the Svecofennian orogen. The thermal relaxation of the crust and the beginning of partial melting may take 20-35 my after crustal thickening i.e. after an arc-continent collision or a terrane accretion (Huerta et al., 1996; Vanderhaeghe and Teyssier, 2001), a stage that is represented in the post-collisional analog models in Papers I and II.

The widespread melting in the middle crust may have facilitated lateral transportation of the middle crust in the Svecofennian orogen (Papers I and II) similarly to the ancient Variscan (Vanderhaeghe et al., 1999) and the present Himalayan orogens (Nelson et al., 1996). A partial melting of ca. 7-10 % is enough to reduce the bulk rock strength and to facilitate flowing (Brown, 2007). In order to generate nearly homogeneous widespread melt and flow in a crustal layer, the melt must form an interconnected network via deformation bands (Brown, 2007) or by melt bearing grain boundaries (Rutter, 1997; Rosenberg and Handy, 2005). A high degree of partial melting requires a high T-environment (650- 800° C depending on rock composition and the amount of H_2O; Brown, 2007). This implies that widespread melting within a crustal layer is visible in a hot orogen environment (e.g. Vanderhaeghe et al., 1999; Vanderhaeghe and Teyssier, 2001), such as the high-T, low-P Svecofennian accretionary orogen (Korsman et al., 1999a) or Variscan orogen (Vanderhaeghe et al., 1999; Gerdes et al., 2000).

In nature, a low-viscous crustal layer, which is able to flow, is far from a homogeneous mass (e.g. Leonov, 2008; Torvela, 2016). A low-viscous flowing layer can have mobile and rigid parts, but if it can deform and flow by lateral flow or by lateral displacement of rock masses, it can be called a flowing layer (Leonov, 2008). In the analog models it is assumed that in nature a heterogeneous, but low viscous, crustal layer was rheologically weak on average, and thus acts in the larger scale as a consistent weak layer.

The average thickness of a middle crust varies from 10 km to 20 km (Mooney et al., 1998), but for example in the Himalayas it is up to 30 km thick (Shapiro et al., 2004). In the Svecofennian orogen in Finland, the middle crust has been interpreted to be 20-30 km thick at present (Korja and Heikkinen, 2008; Korja et al., 2009; Sorjonen-Ward, 2006), although ca. 10 km internal thickness changes can be found (Korja et al., 1993). In the analog models, the middle layers were designed to represent a thicker middle crust than the crust is at present in the Svecofennian orogen.

5.2 Gravitational spreading and middle crustal flow

Gravitational spreading is caused by crustal thickening, which may result in potential energy difference between the thick crust and the adjacent thinner areas (Fig. 7A; Rey et al., 2001). The difference can lead to transportation of crustal material, and cause extension in the thickest parts of the crust. The transportation can occur in the upper crust by normal faulting and by ductile flow in the deep levels of the crust (Rey et al., 2001).

The most common example of flow model, where gravitational pressure component is involved, is channel flow. In channel flow, the low viscous middle or lower crustal layer flows parallel or perpendicular to orogen during collision, and is attached from above and below with more viscous layers (Grujic et al., 1996; Beaumont et al., 2001; Grujic, 2006; Jamieson et al., 2011). In active orogens, the channel flow is driven by the motion of the upper and lower plates and by the lithostatic pressure differences (Grujic, 2006), while the extrusion of the low-viscous material towards the surface is driven by orographic processes (Beaumont et al., 2001). The models presented in Papers I and II have simulated a significant post-collisional/-accretion mid-crustal spreading where free space has been available (Fig. 7D). Although the weakest layer was attached between the stronger ones, the free space, the lack of surface processes and a tunnel type flow show that the models are not directly comparable with a channel flow mode.

Both numerical and analog models suggest that ductile crustal flow is induced by tectonic stresses (Beaumont et al., 2001; Rey et al., 2001; Cagnard et al., 2006), and that the flow direction is more or less parallel in all the crustal layers (and not e.g. orthogonal). Although the flow strike is the same the course of the flow may be opposite, due to velocity differences (shear senses) between the different crustal layers (Grujic, 2006; Godin et al., 2006). The results of Papers I and II support the earlier findings by e.g. Vanderhaeghe et al. (1999), Grujic (2006) and Godin et al. (2006) by emphasizing that the coeval ductile flow is parallel in all crustal layers (Fig. 6B&C).

The pattern of the middle crustal flow in the outcrops is under debate (e.g. Grujic et al., 1996; Cagnard et al., 2007; Brown et al., 2011; Torvela, 2016). The presence of large granitic intrusions or exhumed high-T, low-P migmatites is usually interpreted as a result of high degree of melting (Brown, 1994; Vanderhaeghe et al., 1999; Jamieson et al., 2011). An indication of middle crustal flow is often presented as uplifted gneiss domes or ductile shear zones (e.g. Chardon et al., 2009; Whitney et al., 2004; Vanderhaeghe and Teyssier, 2001), but in the presence of large amount of magmas the flow pattern is magmatic (Vernon, 2000). Altogether the degree of deformation can vary from place to place since the deformation pattern varies with respect to the crustal section and the emplacement level (e.g. Caggianelli et al., 2000; Torvela, 2016). Also the style of deformation can vary from penetrative flow (Beaumont et al., 2001; Jamieson et al., 2006) to combination of block movement, shear zone network and melt transportation (Cagnard et al., 2006; Leonov, 2008, 2012; Torvela et al., 2013; Torvela, 2016). Paper III discusses the results of mid-crustal lateral flow found in batholiths that can consist of gneissic and undeformed plutonic rocks. The flow pattern has been accommodated by magmatic flow, gneissic foliation and localized deformation zones in the CFGC batholith. In crustal scale, the flow has caused gneissic doming (BB; Kyyjärvi dz) and block rotation (IC, OA), and thus changes in the metamorphic grade. The study area (Figs. 4&5), represented by the central part of the Svecofennian orogen discussed in the section 5.5 and in Paper III, suggest that the degree of deformation can vary both regionally but also across the entire orogenic belt.

5.3 The impact of pre-existing components and crustal scale weakness zones

Despite the viscosity difference between the thermomechanical (Paper I) and the centrifuge analog models (Paper II), the results indicate similar crustal deformation. Both experimental set-ups show subsidence and thinning of the upper and the middle crusts, uplift of the middle and lower crusts and extensional and compressional structures (Fig. 6). However, in the thermomechanical analog modeling experiments the compressional component has formed reverse faults (Paper I), whereas in the centrifuge analog modeling experiments the compressional structures has shortened the boundary zone and the subblocks (Paper II). The results suggest that if the extensional stress field is higher than the compressional one and the middle layer is the weakest among the layers, a similar large-scale deformation pattern of the mid-crustal lateral flow is found.

In Paper I it is proposed that the lateral spreading is bottom driven i.e. the deformation starts from the bottom of the crust and advancing upwards. However, it must be emphasized that in both of the modeling experiments the motion has been provided by the flow of the lowest viscosity layer in the middle (Papers I and II). The weakest layer has the highest strain and has controlled the deformation styles of both the upper and the lower layers (Papers I and II). In the models, flow has also occurred along the bottom of perplex box (Paper II) or heated plate (Paper I), hence the lower layer deformation has interacted with high strain flow above and steady bottom. This may explain the formation of domino structures and fractures in the

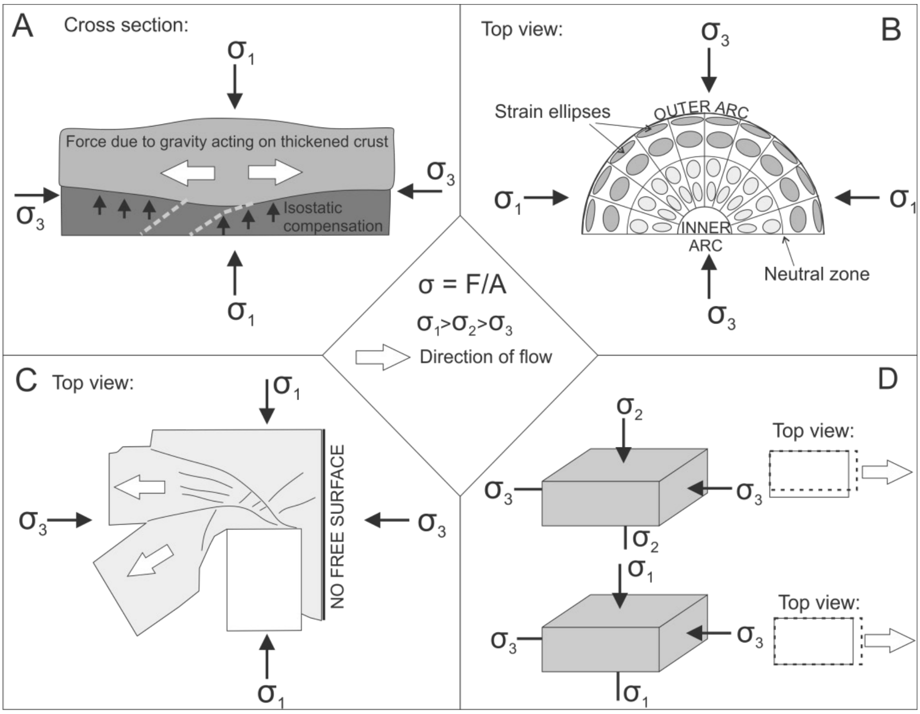

Figure 7. Stress fields of three different post-accretion/collision lateral displacement/flow models and the stress field in the analog models in Papers I and II. A) The lateral variations in gravitational potential energy attempts to level out topographic differences, which may result in extension of a thickened orogen (Rey et al., 2001). Modified after Nemčok et al. (2013). B) Buckling of orocline can cause shortening of the inner arc and stretching of the outer arc. In the neutral zone there is no strain (Ries and Shackleton, 1976). Modified after Weil et al. (2013). C) In collisional zones, shortening can cause tectonic escape of crustal or lithospheric material subparallel (max. 40° of block rotation; Tapponnier et al., 1982) to the convergence direction. Tectonic escape is interpreted to be a part of the collisional zones in the case where one side is blocked. Modified after Tapponnier et al. (1982). D) The principal stress fields of the analog modeling boxes and the change in the model shape in top view during modeling. The thermomechanical analog modeling set-up simulates "orogen parallel flow" (above). The centrifuge analog modeling set-up simulates "orogen perpendicular flow" (below).

lower crust in the thermomechanical analog models (Paper I), suggesting that the lower layer deformed by lateral displacement of crustal blocks instead of continuous flow. In the centrifuge analog models, the bottom has been smeared to avoid friction (Paper II), which may explain the lack of similar semi-brittle behavior.

The cause and consequence of thickness changes of the middle crust has not been discussed in detail in Papers I and II, even though it has been proposed that the middle layer has controlled the deformation. Subsidence and uplift of the upper and the lower layers (Papers I and II) are connected to the thickness changes in the middle layer. When the middle layer thins, the lower layer uplifts and the upper layer subsides, and when the middle layer uplifts or thickens the lower layer thins and the upper layer extends by faulting (Papers I and II). Similar results have also been presented before (e.g. Vanderhaeghe et al., 1999; Koyi and Skelton, 2001; Corti et al., 2003). The interaction between the layers is suggested to explain the moderate net thinning (up to 22 %) during gravitational spreading and an explanation for the thick Svecofennian crust (Paper II).

The results show that the inherited terrane components have a large impact on the style of deformation (Paper II). With pre-existing terrane components, such as two mechanically contrasting blocks, the deformation is concentrated at (and caused elongation of) the block boundary. The final end result is dependent on the rheological properties of the different crustal blocks compared to the flow direction. If the blocks have contrasting rheological properties, the weaker block will flow at a higher rate than the stronger one (Paper II). This results in an elongated and a shallowly dipping terrane boundary, similar to low-angle structures found on FIRE1 and 3a seismic reflection profiles (Paper II). Further, the transportation of the weak layer over the other block can 1) develop a detachment zone at the middle-lower crustal boundary zone (Paper II); 2) form a complex suture zone with a "crocodile" structure (Paper II), which has been proposed for the IC at the Archean margin (FIRE1; Korja and Heikkinen, 2005; 2008; Lahtinen et al., 2015); and/or 3) create crustal layering with significant age differences, which can further generate melts with inherited components such as zircons.

The deformation is more evenly distributed in the models, when the number of pre-existing weakness zones increase (Paper II). With additional terrane boundaries or stacking surfaces, the deformation is not only concentrated on the weakest layer or as elongation of the boundary zone (Fig. 6C), but deformation will also take place in more rigid areas, and thus is not only a regional event (Paper II). These conclusions are in agreement with modeling results by e.g. Rey et al. (2001) and Harris et al. (2012), who proposed that gravitational spreading will deform and extend also adjacent areas. In Paper II, it is shown that the areas adjacent to the weakest crustal component may deform by block rotation, upward flow or subsidence, which may lead to rapid changes in the lithological record of the juxtaposed blocks. The vertical movement can be observed as variations of rock types or metamorphic grade in exhumed orogens such as the Svecofennian orogen (Papers II and III). The distributed deformation (Paper II) in the models indicates that gravitational spreading of an orogen will accommodate along terrane boundaries and into adjacent crustal blocks as well.

5.4 The tectonic setting of the analog models

To evaluate the impact of the pre-existing components, two different modeling methods were used. In both experiments a free space was available to mimic the adjacent thinner area(s) of a thick crust or retreating plate boundary. The models in Paper I represent the syn-compressional stage of a thickened orogenic crust where extension is the main process, thus these models can be compared to active orogenies with ongoing compression. If it is assumed that the compression direction in the models represents the orientation of an orogenic belt, the modeling set-up shows parallel flow of an orogen (Fig. 7D; Paper I). The models in Paper II represent post-compressional stage, with unilateral extension. If it is assumed that the block boundary exemplify the location of a suture zone, the modeling set-up represents flow perpendicular to the orogenic strike (Fig. 7D; Paper II).

The orogen parallel flow can initiate during convergence by tectonic escape (Fig. 7C; Tapponnier et al., 1982; Cagnard et al., 2006; Leonov, 2008). Tectonic escape occurs in active orogenic belts in response to collision-induced shortening, which causes lateral movements parallel to the orogenic strike (Tapponnier et al., 1982; Ching et al., 2007; Leonov, 2008). Characteristic for the tectonic escape is that only one boundary is free (Tapponnier et al., 1982; Cagnard et al., 2006). The modeling set-up in Paper I represented orogen parallel flow. Only minor shortening (compared to elongation) was involved, whereas elongation was a predominant feature. However, the term tectonic escape could be used when describing the set-up of the models in Paper I, but it also should be noted that the "stress field" is not the traditional one. Hence, the results of the structures of the models in Paper I differ from those interpreted from the tectonic escape model presented earlier (Tapponnier et al., 1982; Cagnard et al., 2006).

Tectonic escape will generate major strike-slip and transpressive faults, and horizontal flow (Fig. 7C; Tapponnier et al., 1982; Leonov, 2008; Cagnard et al., 2006), as well as flower structures and thickening of the crust (Cagnard et al., 2006). The deformation in the CFGC at 1.89 Ga and younger has been interpreted to be transtensional or extensional (Nironen et al., 2000; Nironen, 2003; Lahtinen et al., 2005; Paper III), and contains lateral flow of the middle crust (perpendicular to the tectonic boundary in the west of the CFGC; Korja et al., 2009; Papers I and II). Also, the thick crust of the CFGC has been suggested to have thinned after the compression (Lahtinen et al., 2005; Kukkonen et al., 2008; Korja et al., 2006; 2009; Papers I and II), not thickened, like the tectonic escape model suggests. The lack of traditional structures interpreted in the tectonic escape models suggests that the model does not explain the post-accretion deformation in the CFGC.

5.5 The evolution of the central part of the Svecofennian orogen between 1910 Ma and 1870 Ma

The central part of the Svecofennian orogen has a thick three-layer crust (Grad and Luosto, 1994; Luosto and Heikkinen, 2001; Korja et al., 1993; Kozlovskaya et al., 2004). It has been argued that three-layer crustal structure in mature island arcs and microcontinents with intermediate to felsic middle crust were formed prior to accretion or collision (e.g. Mooney et al., 1998; Tetreault and Buiter, 2014). This argues for a three-layer crustal structure prior to accretion also in the Svecofennian orogen, and that the syn- and post-accretion crustal differentiation only enhanced the pre-existing layered crust.

5.5.1 1910-1890 Ma

The Svecofennian accretionary orogen commenced at 1.91 Ga (Lahtinen et al., 2005), and the oldest post-accretional rocks are ca. 1.89 Ga (e.g. Nironen, 2003; Paper III), suggesting a thermal relaxation period of 20 my (Fig. 8).

5.5.2 1890-1884 Ma

The age and the composition of magmatic rocks in the Paleoproterozoic part of the Svecofennian orogen suggest that the Group 1 rocks have been generated from calcic partial melts forming in the lower crust after terrane accretion (Fig. 8B; Nironen et al., 2000; Paper III) and that they were emplaced before 1887 Ma (Paper III). Magmas are transported and emplaced on shallow crustal levels, but they can also be trapped by the brittle-ductile transition zones, by other tectonic structures, or shear zones (D'Lemos et al., 1992; Brown, 1994, 2007). The Group 1 magmas are suggested to be arrested in the upper crust (Paper III), but some melts may have been trapped in the middle crust facilitating partial melting and generation of Group 2 magmas.

The widespread melting and weakening in the middle crust and the subsequent formation of Group 2 magmas has started at 1890 Ma. The (sub)volcanic rocks (Group 2) have subsided before the emplacement of the granodiorites at 1884-1883 Ma, shown by cross-cutting relationships in the Kalmari complex (Fig. 5; Paper III). The thermomechanical modeling indicates that the upper crustal blocks can subside concurrently with the extension if the layer below is weak enough (Paper I). This suggests that when the granodiorites have been emplaced, the melting of the middle crust had already enabled subsidence and extension. The previous studies have proposed an extensional event at ca. 1880 Ma (Nironen et al., 2000; Nironen, 2003; Papers II) and at ca. 1884 Ma (Paper III) in the CFGC. The latter one is more likely due to the subsidence and the existence of the weak middle crust, and the cross-cutting relationship. These can imply that the extensional stage

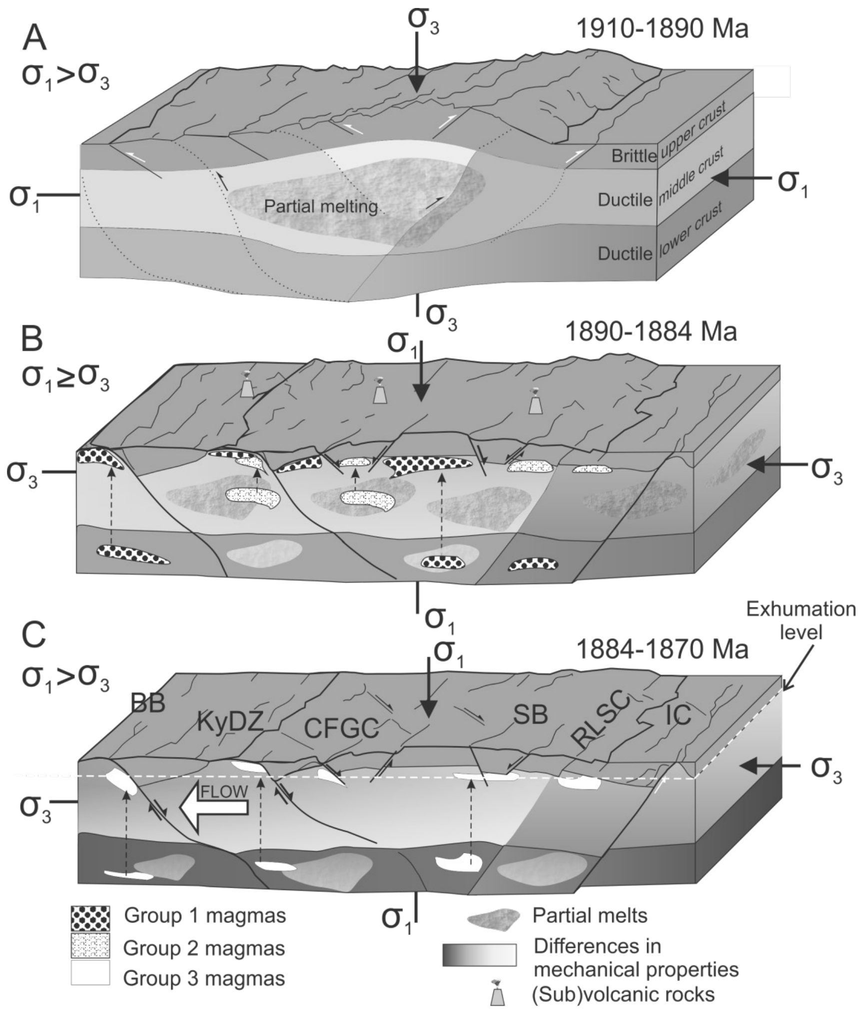

Figure 8. A conceptual 3D evolutionary model for the central part of the Svecofennian orogen at 1910-1870 Ma. A) Terrane accretion had juxtaposed components with different mechanical properties together. The collage has inherited shear zones and a three-layer crust. Between 1910-1890 Ma partial melting took place in the lower and the middle crusts. B) The principal stress changed from horizontal to vertical due to GPE difference in the orogenic belt. The partially molten layer in the middle crust facilitated exhumation and lateral spreading, which reactivated the tectonic contacts and the shear zones. Group 1 magmas formed in the lower crust and accommodate at shallow levels. Group 2 magmas formed in the middle crust and rose to surface and erupted as (sub)volcanic rocks at 1890-1886 Ma and to upper part of the middle crust and emplaced as granodiorites at 1886-1883 Ma. C) The gravitational spreading started at ca. 1884 Ma. At that time Group 3 magmas formed in the lower crust. The magmas transported to the upper and the middle crusts via the pre-existing tectonic contacts and the shear zones. The inherited structures tilted and extended during the one-way gravitational spreading and the middle crustal flow. The spreading took place as block rotation of the IC, thinning of the middle crust below the CFGC and the dome structure of the BB. Kyyjärvi deformation zone was reactivated between 1880-1870 Ma. Abbreviations: *IC – Iisalmi complex; BB – Bothnian belt; CFGC – Central Finland granitoid complex; KyDZ – Kyyjärvi deformation zone; RLSC – Raahe-Ladoga shear complex; SB – Savo belt.*

may have started even before 1884 Ma, between the formation of the (sub) volcanic rocks and granodiorites in the CFGC.

5.5.3 1884-1880 Ma

The Group 3 bimodal magmas were emplaced at 1881-1880 Ma in a less ductile environment than the Group 2 granodiorites a few my earlier (Fig. 8C; Nironen et al., 2000; Paper III). Kukkonen et al. (2008) proposed ca. 8 km difference in the emplacement depths between the granodiorites (Group 2) and the granites (Group 3). Elliott et al. (1998) have modeled that these granites were emplaced at 0.2-0.4 GPa and tonalites and/or granodiorites at 0.5 GPa, indicating less than 8 km difference in the emplacement levels between Groups 2 and 3, and an exhumation rate of 1.3-2.7 mm/y. Nevertheless, both studies proposed exhumation after crystallization of Group 2 rocks. If Group 3 rocks were associated with extensional or transtensional events (Nironen et al., 2000; Nironen, 2003; Paper III), then exhumation prevailed also during the emplacement at 1881-1880 Ma.

Gravitational spreading is proposed to have reactivated pre-existing surfaces (Paper II), which guided the transportation of the Group 3 magmas from the H_2O poor lower crust (Nironen et al., 2000; Papers II and III). Localized SE-NW trending subvertical shear zones are proposed as transport zones having been reactivated during and after the emplacement of the Group 3 rocks (Nironen et al., 2000; Nironen, 2003). These shear zones are mainly present in the upper part of the middle crust (Korja et al., 2009; Paper III), but some of them have been interpreted to continue to lower crust (Lahtinen et al., 2009). In contrast, wide mylonitic deformation zones such as Kyyjärvi deformation zone (Sorjonen-Ward, 2006; Korja et al., 2009), which was still active after 1880 Ma (Paper III), and the boundary between BB and CFGC, represent larger reactivated tectonic surfaces, which reach deeper crustal levels (Paper II). These shear zones are more likely candidates for the melt transport from the lower crust to emplacement in the middle-upper crust.

5.5.4 1880-1870 Ma

The timing of the deformation is inferred from the age of the plutons. Group 3 plutons at ca. 1880 Ma are cross-cut by localized shear zones, the Kyyjärvi deformation zone and Elämäjärvi detachment zone in the CFGC (Rämö et al., 2001; Nironen, 2003; Vaarma and Pipping, 2003; Kilpeläinen et al., 2008; Paper III). The deformation in the northern CFGC was active after at 1875 Ma (Lahtinen et al., 2015) until 1860 Ma (Kilpeläinen et al., 2008). The estimation of the termination of the extensional deformation was based on the activity of the Elämäjärvi detachment zone (Kilpeläinen et al., 2008). The error limits of the U-Pb zircon age of the granite cross-cut by the Elämäjärvi detachment zone (A1122:1867 ± 12 Ma; Kousa et al., 1994) indicate that the emplacement of the granite and the development of the Elämäjärvi detachment zone could have taken place already ca. 1880 Ma. This is supported by earlier studies proposing that the deformation has been active at 1880-1870 Ma within the CFGC (Lahtinen et al., 2005; Korja et al., 2006), and by studies which have concluded that the plutonic rocks at 1880 Ma have undergone deformation soon after their emplacement (Anttila et al., 1992; Paper III). This makes it unlikely that the ductile deformation, which reactivated the shear zones, could be as young as 1860 Ma in the CFGC, but it implies that the extensional stage was active until 1870 Ma (Fig. 8C).

5.6 The gravitational spreading in the Svecofennian orogen

Several processes have been proposed for the exhumation and the deformation in the CFGC: 1) gravitational or extensional collapse (Lahtinen et al., 2005; Korja et al., 2006, Paper I), 2) an upper crustal collapse (Kukkonen et al., 2008), 3) lateral spreading (Korja et al., 2009), or gravitational spreading (Paper II), and 4) a buckled orocline (Lahtinen et al., 2014). All the proposed processes have been suggested to have taken place between 1880 Ma and 1860 Ma. Also younger events (1850 Ma; Sorjonen-Ward, 2006; Kukkonen et al., 2008) have been proposed but those are not discussed here. In processes 1-3 the maximum principal stress field (σ_1) is subvertical, whereas in process 4, σ_1 is subhorizontal (Fig. 9).

In the buckled Bothnian orocline model, a linear Svecofennian orogenic belt is bent and folded, which results in squeezing the CFGC between the Archean margin, the SB and the BB at 1870-1860 Ma in NW-SE shortening (σ_1 in Fig. 9D; Lahtinen et al., 2014). The model, which is based on review of previous studies, infers that the CFGC has rotated during buckling resulting from compression. The buckling would cause shortening of the inner arc and elongation of the outer arc regions, and strike-slip shear zones parallel to the buckling (Fig. 7B; e.g. Ries and Shackleton, 1976; Weil et al., 2013). Shear zones parallel to the suggested buckling have not yet been found in the CFGC. Furthermore, field observations (Nironen et al., 2000; Nironen, 2003; Paper III) show that the structures between 1884 Ma and 1870 Ma in the CFGC have rather been formed in an extension/transtension, with vertical σ_1.

The gravitational spreading models in the CFGC differ from each other by vertical dimensions, stress fields and flow directions (Lahtinen et al., 2005; Korja et al., 2006; 2009; Kukkonen et al., 2008; Papers I-III). The stress fields are interpreted in Figure 9. Lahtinen et al. (2005) and Korja et al. (2006) suggested minor collapse and spreading towards the south at 1.87 Ga in the CFGC (Fig. 9B; σ_1:vertical$_;$ σ_3:N-S). Korja et al. (2009) suggested large-scale lateral spreading in N-S, NW-SE and westward directions (σ_1:vertical$_;$ $\sigma_1 > \sigma_2 = \sigma_3$) at 1.88-1.87 Ga. Whereas Kukkonen et al. (2008) suggested that the upper crustal collapse occurred in NNW-SSE direction (σ_3) at 1.88-1.87 Ga, in the same direction as shortening (σ_1) few my earlier, at 1.89 Ga (Fig. 9C). All authors have interpreted that the gravitational spreading changed the stress field between 1.89 Ga and 1.88-1.87 Ga. However, the direction and the depth of the lateral flow vary between the authors, although all agree that the flow was not towards the east. Based on field evidence (Nironen et al., 2000; Nironen, 2003; Paper III; Lahtinen et al., 2016), the thesis suggests changes in the stress fields from lateral compression to extension at ca. 1884 Ma (Fig. 9E).

In the CFGC, the flow or the crustal movement at the present surface has been proposed to be in a E-W to NW-SE direction at 1890-1870 Ma (Fig. 8; Nironen et al., 2000; Korja et al., 2009; Papers II and III), indicated by the orientation of the subvertical strike-slip shear zones (Nironen et al., 2000) and the dominant subhorizontal lineation (Kilpeläinen et al., 2008). As discussed before, the flow is subparallel in all crustal layers, suggesting that the flow

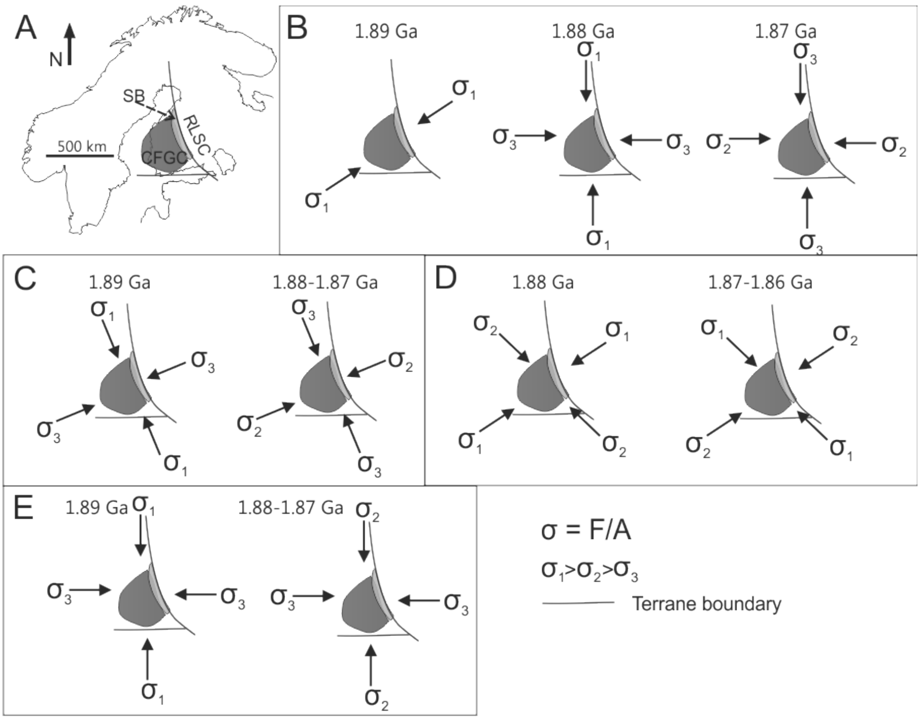

Figure 9. Different interpretations of the stress fields around the Central Finland granitoid complex (CFGC), between 1.89 Ga and 1.87 Ga, found in literature. To simplify the presentation of the stress fields in B- E, the tectonic model in A is used in all interpretations, although the shape and the volume is expected to change along with the changing of the stress fields. A) A tectonic model of the location of the CFGC, the Savo belt SB and the Raahe-Ladoga shear complex (RLSC) at 1.89 Ga (modified after Lahtinen et al., 2005). The stress fields are caused by: B) Microcontinent accretion and minor gravitational collapse (Lahtinen et al., 2005; Korja et al., 2006); C) Arc collision and upper crustal collapse (Kukkonen et al., 2008); D) Buckling of an orocline (Lahtinen et al., 2014); E) Terrane accretion and gravitational spreading (this thesis).

direction at surface marks also the flow deeper in the crust. The ductile flow is usually described by mineral lineations (e.g. Solar et al., 1998; Vernon, 2000). In the CFGC, the lineation can be divided into two categories: E-W stretching lineation (Kilpeläinen et al., 2008) and SE-NW directed slickenside (Korja et al., 2009; Paper III). The lineations indicate mainly flow (or stretching) in the E-W and the NW-SE directions (σ_3) in the northern and the central part of the CFGC.

A N-S horizontal shortening after 1890 Ma has been proposed by Nironen (2003) and Sorjonen-Ward (2006), which can explain both lineations. The stretching lineation is found in rocks of 1890 Ma and younger. The SE-NW slickenside lineation is found in the SE-trending, oblique slip shear zones, which are younger than 1880 Ma (e.g. Nironen et al., 2000). The change in the style of deformation from pervasive <1890 Ma (stretching lineation) to localized <1880 Ma (slickenside lineation) under the same horizontal shortening direction supports the models with active exhumation between 1890-1880 Ma. The deformation of the exhumed rocks can be changed from ductile penetrative to localized in the shear zones when the P-T environment changed.

Between 1890 Ma and 1870 Ma concurrent deformation and magmatism occurred in the central part of the Svecofennian orogen, forming for instance the CFGC. The Paleoproterozoic deformation and magmatism in the RLSC, the IC and the OA are mainly younger than 1890 Ma (e.g. Huhma, 1986; Paavola, 1987; Hölttä et al., 2000; Sorjonen-Ward, 2003; Lahtinen et al., 2015). Plutonic rocks formed between 1890 Ma and 1860 Ma (Paavola, 1987; 1988; Huhma, 1986; Ruotoistenmäki, 2001) in the IC, the RLSC and the CFGC. The NW-trending shear zones developed after 1900 Ma (Hölttä and Paavola, 2000) in the IC and the RLSC, and after 1880 Ma in the CFGC. The OA and the Pyhäsalmi deformed between 1880 Ma and 1860 Ma (Sorjonen-Ward, 2003) and <1875 Ma (Lahtinen et al., 2015), respectively. It was proposed in Paper II that the RLSC was reactivated and crustal block rotated the IC and the OA during the westward gravitational spreading. The ductile deformation and the magmatism in the BB, the CFGC, the IC, the OA and the RLSC post-date the terrane accretion at 1910 Ma (Lahtinen et al., 2005), proposing to be caused by post-accretion processes. The coeval ductile deformation and exhumation in the BB, the CFGC, the RLSC, the IC and the OA, the reactivation of pre-existing structures, the coeval extensional and compressional structures, and the three magmatic groups across the central part of the Svecofennian orogen can be explained by one simple process - the gravitational spreading.

The analog models suggest the gravitational spreading has lasted for 16-23 my and the crust has extended by ca. 50 % (Paper II). The duration of the spreading is closer to 16 my, if pre-existing weakness zones are present (Paper II). The results of the duration of the spreading are comparable the interpretations (10-25 my) from the Paleoproterozoic side of the Svecofennian orogen in Finland (Paper III). Because reactivated pre-existing surfaces are present in the CFGC, the duration is most likely on the shorter side of this time interval. The exhumation has commenced ca. 1884 Ma and ductile deformation continued until 1870 Ma, which suggest that the gravitational spreading has been ongoing for 16-14 my in this part of the orogen.

5.7 General discussion and future studies

The study suggests that the gravitational spreading is an efficient crustal deforming process in lateral and vertical directions across the orogen. This research has focused on studying structures, which have formed via gravitational spreading. It will help in distinguishing the syn-collision extensional structures from the post-collisional extensional ones. The lateral spreading of a weak middle crust can lead to coeval normal and reverse faults, or to major tilting and rotation of blocks, and to breaking and discontinuation of structures. All the observations could also be interpreted as two separate deformational events instead of only one with multiple forms. It is important to separate the effect of gravitational spreading on syn-collisional structures. It will help in to avoid confusing interpretations and help in simplification of the interpretations of post-collisional/-accretional crustal evolution.

In this thesis, the crustal deformation was studied by analog models, and the geochronological, the geochemical and the geophysical data were used to compare the analog models to nature. In the study area, there were several interpretations of the post-accretion evolution and the direction of the flow (Lahtinen et al., 2005; 2014; Korja et al., 2006; 2009; Kukkonen et al., 2008). To approach this problem one of the challenges was to define the age of the deformation. Since the study area consists mainly of magmatic rocks (without any metamorphic indication minerals), and indication minerals were not found from the sampled shear zones, magmatic U-Pb ages were used to get the relative age of the deformation. The typical rock types were identified by geochemistry and petrography to improve the magmatic evolution model, and using that the deformation events were separated from the magmatic ages. Although structural data were available from earlier studies and Paper III, more detailed structural analysis would improve the post-accretion evolution model and the movement of the flow in the CFGC. Hence, structural analysis could resolve the varying interpretations of the stress fields found in the literature at present.

6 Concluding remarks

This study has modeled late orogenic event by two sets of analog modeling experiments. The results have been compared to new geochronological and geochemical data sets and to crustal scale seismic profiles in the central part of the Svecofennian orogen. The main findings can be summarized as follows:

Thick orogenic crust with a ductile middle layer undergoes lateral spreading at all crustal layers if free space is available. The spreading will propagate to adjacent areas across the orogenic belt or the tectonic boundaries. The spreading is facilitated by pre-existing terrane boundaries and thick-skin stacking surfaces.

In an over-thickened three-layer crust, lateral spreading produces elongation and shortening of terrane boundaries, stacking surfaces, crustal layers and blocks, normal and reverse faults, block tilting, ductile thinning and thickening of crustal layers. The normal faults and the elongation of the layers and the stacking surfaces are predominant features, although local shortening structures or reverse faults can be formed as well. The results show that a tectonic boundary cannot resist lateral spreading.

Thermal relaxation took ca 20 my in the central part of the Svecofennian orogen. The exhumation and the lateral spreading started at ca. 1884 Ma, continuing until 1870 Ma. Hence the gravitational spreading was active 16-14 my and it elongated the crust by approximately 50 % at that time. Ongoing exhumation has changed the deformation pattern in the plutonic rocks from pervasive, gneissic structures to localized shear zones in the Central Finland granitoid complex. The coeval exhumation, the lateral spreading and the magmatism of the central part of the Svecofennian orogen is best explained by westward gravitational spreading.

Acknowledgement

The topic of this research has been multidisciplinary within geology and has continued for long time, why there's plenty of people I want to thank.

First of all I want to thank my supervisors who believed in my skills even before I did: my supervisor Prof. Olav "Joffi" Eklund for his positive and motivating attitude; my supervisor Dos. Annakaisa Korja for introducing me to the dark side of geology, to geophysics, and for the time she always had for me to discuss, or read and polish my writing work.

I'm truly thankful to all my co-authors, especially i) Prof. Hemin Koyi for his supervision at the Hans Ramberg analog modeling laboratory and for the many serious and the less serious discussions during the years; ii) Dr Carlo Dietl who introduced me in the world of analog modeling; iii) Dr. Irmeli Mänttäri who more than helped with the geochronological data and gave always so positive feedback; iv) Dr. Baishali S Roy Chowdhury, who helped me in the Laboratory in Frankfurt am Main and drafted the manuscript; and v) Dr. Mikko Nironen who was so open minded during manuscript work.

I sincerely thank Dr. Paula Kosunen, who carried out an important part of the field work, and whose data we've also used in the last Paper.

I would like to thank the MIDCRUST-project members and the people who participated in the meetings and the excursion, especially Dr. Francis Chopin, Prof. Tapani Rämö, Dr. Matti Kurhila, Prof. Toivo Korja, and Dr. Pentti Hölttä.

I would like to thank Prof. David Whipp with the discussions we had on geodynamic models and modeling. He had a large impact to improve my understanding of geodynamic modeling.

I could thank Prof. Pietari Skyttä for many reasons, but maybe I'm most thankful for one discussion long time ago about the contents of the manuscripts.

For precious comments to this thesis I would like to thank Dr. Johanna Salminen, Dr. Karin Högdahl and MSc/Dr. Elina Lehtonen. And for language checking I would like to thank Dr. Timothy Wilson, MSc Anna Saukko and MSc Jon Engström.

The colleagues at the Institute of Seismology, you all rock, although you don't know a lot about geology ("Vitsi, vitsi" as someone would say at the coffee table). I know I was the black sheep, but I managed so far, and I've left stinky stickers for your pleasure. Deal with it!

I'm grateful for having such great colleagues in the Åbo Akademi University, present and formers, who always made me feel that I belong to ÅA although I visited there rarely.

The many colleges, especially Dr. Seija Kultti, MSc Elina Lehtonen, MSc Henrik Kalliomäki, Dr. Suvi Heinonen, MSc Niina Hellqvist, MSc Ilmari Smedberg, MSc Sonja Lavikko, and Dr Susanna Kihlman, I would like to thank you all for the peer-support in the form of many discussions, reviewing, and listening. Without you this process would have been harder.

I am grateful to the reviewers, Dr. Giacomo Corti and Dr. Taija Torvela, for their valuable comments that helped to improve the thesis.

The financial support has been provided by Academy of Finland through MIDCRUST-project, K.H Renlunds foundation, Väisälä foundation, and Rector of Åbo Akademi University. Thank you.

At the end, I would like to thank my family, my Mom and Dad, who have always listened me during my journey. I'm more than grateful to my mother- and father-in-laws, Merja and Erkki, who never declined the request to take care of our children. My dear husband Mikko, this would not have been possible without your support in every sense of the word. You have always encouraged and helped me, even though the process seemed quite endless at some point(s). Thank you for being in my life! And in the end I want to thank my two apes, Elias and Aaro alias rötvä and pötkylä, for just existing, because I would not be me without you two!

Vantaa 23.08.2016 Kaisa Nikkilä

References

Anttila, P.(ed)., Paulamäki, S., Lindberg, A., Paananen, M., Koistinen, T., Front, K., Pitkänen, P., 1992. The Geology of the Kivetty Area, Summary Report. Nuclear Waste Commission of Finnish Power Companies 07.

Beaumont, C., Ellis, S., Pfiffner, A., 1999. Dynamics of sediment subduction-accretion at convergent margins: Short-term modes, long-term deformation, and tectonic implications. Journal of Geophysical Research: Solid Earth 104 (B8), 17573-17601.

Beaumont, C., Jamieson, R.A., Nguyen, M.H., Lee, B., 2001. Himalayan tectonics explained by extrusion of a low-viscosity crustal channel coupled to focused surface denudation. Nature 414 (6865), 738-742.

Beaumont, C., Jamieson, R.A., Nguyen, M.H., Medvedev, S., 2004. Crustal channel flows: 1. Numerical models with applications to the tectonics of the Himalayan-Tibetan orogen. Journal of Geophysical Research: Solid Earth 109 (B6), - B06406.

Brown, L.D., Zhao, W., Nelson, K.D., Hauck, M., Alsdorf, D., Ross, A., Cogan, M., Clark, M., Liu, X., Che, J., 1996. Bright Spots, Structure, and Magmatism in Southern Tibet from INDEPTH Seismic Reflection Profiling. 274, 688-690.

Brown, M., 2007. Crustal melting and melt extraction, ascent and emplacement in orogens: mechanisms and consequences. Journal of the Geological Society 164 (4), 709-730.

Brown, M., 1994. The generation, segregation, ascent and emplacement of granite magma: the migmatite-to-crustally-derived granite connection in thickened orogens. Earth-Sci. Rev. 36 (1–2), 83-130.

Brown, M., Korhonen, F.J., Siddoway, C.S., 2011. Organizing Melt Flow through the Crust. Elements 7 (4), 261-266.

Burg, J., Ford, M., 1997. Orogeny through time: an overview. Geological Society, London, Special Publications 121 (1), 1-17.

Caggianelli, A., Prosser, G., Rottura, A., 2000. Thermal history vs. fabric anisotropy in granitoids emplaced at different crustal levels: an example from Calabria, southern Italy. Terra Nova 12 (3), 109-116.

Cagnard, F., Durrieu, N., Gapais, D., Brun, J., Ehlers, C., 2006. Crustal thickening and lateral flow during compression of hot lithospheres, with particular reference to Precambrian times. Terra Nova 18 (1), 72-78.

Cagnard, F., Gapais, D., Barbey, P., 2007. Collision tectonics involving juvenile crust: The example of the southern Finnish Svecofennides. Precambrian Res. 154 (1–2), 125-141.

Cawood, P.A., Kroner, A., Pisarevsky, S., 2006. Precambrian plate tectonics: criteria and evidence. GSA today 16 (7), 4.

Cawood, P.A., Kröner, A., Collins, W.J., Kusky, T.M., Mooney, W.D., Windley, B.F., 2009. Accretionary orogens through Earth history. Geological Society, London, Special Publications 318 (1), 1-36.

Chardon, D., Gapais, D., Cagnard, F., 2009. Flow of ultra-hot orogens: A view from the Precambrian, clues for the Phanerozoic. Tectonophysics 477 (3–4), 105-118.

Ching, K., Rau, R., Lee, J., Hu, J., 2007. Contemporary deformation of tectonic escape in SW Taiwan from GPS observations, 1995–2005. Earth Planet. Sci. Lett. 262 (3–4), 601-619.

Chowdhury, B.R., Dietl, C., Zulauf, G., Peinl, M., Zanella, F., 2009. A new thermomechanical deformation apparatus for 3D coaxial deformation and its application to rheologically stratified models. Geotectonic Research 96 (1), 3-19.

Collins, W.J., 2002. Hot orogens, tectonic switching, and creation of continental crust. Geology 30 (6), 535-538.

Condie, K.C., 2014. Growth of continental crust: a balance between preservation and recycling. Mineralogical Magazine 78 (3), 623-637.

Condie, K.C., 1973. Archean Magmatism and Crustal Thickening. Geological Society of America Bulletin 84 (9), 2981-2992.

Corrigan, D., 2012. Paleoproterozoic crustal evolution and tectonic processes: Insights from the Lithoprobe program in the Trans-Hudson Orogen, Canada. In: Percival, J.A., Cook, F.A. and Clowes, R.M. (Eds.), Tectonic Styles in Canada: The LITHOPROBE Perspective. Geological Association of Canada, Special Paper 49.

Corrigan, D., Pehrsson, S., Wodicka, N., De Kemp, E., 2009. The Palaeoproterozoic Trans-Hudson Orogen: a prototype of modern accretionary processes. Geological Society, London, Special Publications 327 (1), 457-479.

Corti, G., Bonini, M., Conticelli, S., Innocenti, F., Manetti, P., Sokoutis, D., 2003. Analogue modelling of continental extension: a review focused on the relations between the patterns of deformation and the presence of magma. Earth-Sci. Rev. 63 (3–4), 169-247.

Corti, G., Bonini, M., Innocenti, F., Manetti, P., Mulugeta, G., 2001. Centrifuge models simulating magma emplacement during oblique rifting. Journal of Geodynamics 31 (5), 557-576.

Coward, M.P., 1996. Balancing sections through inverted basins. Geological Society, London, Special Publications 99 (1), 51-77.

Culshaw, N.G., Beaumont, C., Jamieson, R.A., 2006. The orogenic superstructure-infrastructure concept: Revisited, quantified, and revived. Geology 34 (9), 733-736.

D'Lemos, R.S., Brown, M., Strachan, R.A., 1992. Granite magma generation, ascent and emplacement within a transpressional orogen. Journal of the Geological Society 149 (4), 487-490.

Elliott, B.A., Rämö, T.,O., Nironen, M., 1998. Mineral chemistry constraints on the evolution of the 1.88–1.87 Ga post-kinematic granite plutons in the Central Finland Granitoid Complex. Lithos 45 (1–4), 109-129.

England, P.C., Thompson, A., 1986. Some thermal and tectonic models for crustal melting in continental collision zones. Geological Society, London, Special Publications 19 (1), 83-94.

Fossen, H., Rykkelid, E., 1992. Postcollisional extension of the Caledonide orogen in Scandinavia: Structural expressions and tectonic significance. Geology 20 (8), 737-740.

Frisch, W., Dunkl, I., Kuhlemann, J., 2000. Post-collisional orogen-parallel large-scale extension in the Eastern Alps. Tectonophysics 327 (3–4), 239-265.

Gerdes, A., Wörner, G., Henk, A., 2000. Post-collisional granite generation and HT–LP metamorphism by radiogenic heating: the Variscan South Bohemian Batholith. Journal of the Geological Society 157 (3), 577-587.

Godin, L., Grujic, D., Law, R.D., Searle, M.P., 2006. Channel flow, ductile extrusion and exhumation in continental collision zones: an introduction. Geological Society, London, Special Publications 268 (1), 1-23.

Goleby, B.R., Shaw, R.D., Wright, C., Kennett, B.L., Lambeck, K., 1989. Geophysical evidence for 'thick-skinned' crustal deformation in central Australia. Nature 337 (6205), 325-330.

Grad, M., Luosto, U., 1994. Seismic velocities and Q-factors in the uppermost crust beneath the SVEKA profile in Finland. Tectonophysics 230 (1–2), 1-18.

Grad, M., Tiira, T., ESC Working Group, 2009. The Moho depth map of the European Plate. Geophysical Journal International 176 (1), 279-292.

Grujic, D., 2006. Channel flow and continental collision tectonics: an overview. Geological Society, London, Special Publications 268 (1), 25-37.

Grujic, D., Casey, M., Davidson, C., Hollister, L.S., Kündig, R., Pavlis, T., Schmid, S., 1996. Ductile extrusion of the Higher Himalayan Crystalline in Bhutan: evidence from quartz microfabrics. Tectonophysics 260 (1–3), 21-43.

Halla, J., 2005. Late Archean high-Mg granitoids (sanukitoids) in the southern Karelian domain, eastern Finland: Pb and Nd isotopic constraints on crust–mantle interactions. Lithos 79 (1–2), 161-178.

Harris, L.B., Koyi, H.A., 2003. Centrifuge modelling of folding in high-grade rocks during rifting. J. Struct. Geol. 25 (2), 291-305.

Harris, L.B., Godin, L., Yakymchuk, C., 2012. Regional shortening followed by channel flow induced collapse: A new mechanism for "dome and keel" geometries in Neoarchaean granite-greenstone terrains. Precambrian Res. 212-213, 139-154.

Hjelt, S.E., Korja, T., Kozlovskaya, E., Lahti, I., Yliniemi, J., BEAR, SVEKALAPKO Seismic Tomography Working Groups, 2006. Electrical conductivity and seismic velocity structures of the lithosphere beneath the Fennoscandian Shield. Geological Society, London, Memoirs 32 (1), 541-559.

Holdsworth, R.E., Butler, C.A., Roberts, A.M., 1997. The recognition of reactivation during continental deformation. Journal of the Geological Society 154 (1), 73-78.

Hölttä, P., 2013. Svecofennian metamorphism in Pohjanmaa, western Finland. Geological Survey of Finland, Report of Investigation 198, 62-64.

Hölttä, P., Heilimo, E., Huhma., H., Juopperi, H., Kontinen, A., Konnunaho, H., Lauri, L., Mikkola, P., Paavola, J., Sorjonen-Ward, P., 2012. Archaean complexes of the Karelia Province in Finland. Geological Survey of Finland Special Paper (54), 9-20.

Hölttä, P., 1988. Metamorphic zones and the evolution of granulite grade metamorphism in the early Proterozoic Pielavesi area, central Finland. Geological Survey of Finland, Bulletin - Bulletin de la Commission Géologique de Finlande 344.

Hölttä, P., Huhma, H., Mänttäri, I., Paavola, J., 2000. P–T–t development of Archaean granulites in Varpaisjärvi, Central Finland: II. Dating of high-grade metamorphism with the U–Pb and Sm–Nd methods. Lithos 50 (1–3), 121-136.

Hölttä, P., Paavola, J., 2000. P–T–t development of Archaean granulites in Varpaisjärvi, Central Finland: I. Effects of multiple metamorphism on the reaction history of mafic rocks. Lithos 50 (1–3), 97-120.

Huerta, A.D., Royden, L.H., Hodges, K.V., 1996. The Interdependence of Deformational and Thermal Processes in Mountain Belts. Science 273 (5275), 637-639.

Huhma, H., 1986. Sm-Nd, U-Pb and Pb-Pb isotopic evidence for the origin of the Early Proterozoic Svecokarelian crust in Finland. Geological Survey of Finland Bulletin 337, 1-48.

Hyvönen, T., Tiira, T., Korja, A., Heikkinen, P., Rautioaho, E., 2007. A tomographic crustal velocity model of the central Fennoscandian Shield. Geophysical Journal International 168 (3), 1210-1226.

Jackson, J.A., 1980. Reactivation of basement faults and crustal shortening in orogenic belts. Nature 283 (5745), 343-346.

Jagoutz, O., Schmidt, M.W., 2012. The formation and bulk composition of modern juvenile continental crust: The Kohistan arc. Chem. Geol. 298–299, 79-96.

Jamieson, R.A., Beaumont, C., Warren, C., Nguyen, M., 2010. The Grenville Orogen explained? Applications and limitations of integrating numerical models with geological and geophysical data. Canadian Journal of Earth Sciences 47 (4), 517-539.

Jamieson, R., Beaumont, C., Nguyen, M.H., Grujic, D., 2006. Provenance of the Greater Himalayan Sequence and associated rocks: predictions of channel flow models. Geological Society, London, Special Publications 268 (1), 165-182.

Jamieson, R.A., Beaumont, C., 2013. On the origin of orogens. Geological Society of America Bulletin 125 (11-12), 1671-1702.

Jamieson, R.A., Beaumont, C., 2011. Coeval thrusting and extension during lower crustal ductile flow? Implications for exhumation of high-grade metamorphic rocks. J. Metamorph. Geol. 29 (1), 33-51.

Jamieson, R.A., Unsworth, M.J., Harris, N.B.W., Rosenberg, C.L., Schulmann, K., 2011. Crustal Melting and the Flow of Mountains. Elements 7 (4), 253-260.

Kähkönen, Y., 2005. Chapter 8 Svecofennian supracrustal rocks. Developments in Precambrian Geology, Elsevier 14, 343-405.

Kilpeläinen, T., Korja, A., Paavola, J., 2008. Elämäjärven hiertovyöhyke, osa II–lineaatiot ja kuoren kehitystulkinta. Geologi 2, 33-42.

Kontinen, A., Paavola, J., Lukkarinen, H., 1992. K-Ar Ages of Hornblende and Biotite from Late Archaean Rocks of Eastern Finland: Interpretation and Discussion of Tectonic Implications. Geologian tutkimuskeskus, Espoo.

Korja, A., Korja, T., Luosto, U., Heikkinen, P., 1993. Seismic and geoelectric evidence for collisional and extensional events in the Fennoscandian Shield implications for Precambrian crustal evolution. Tectonophysics 219 (1–3), 129-152.

Korja, A., Heikkinen, P., 2005. The accretionary Svecofennian orogen insight from the BABEL profiles. Precambrian Res. 136 (3-4), 241-268.

Korja, A., Heikkinen, P.J., 2008. Seismic images of Paleoproterozoic microplate boundaries in the Fennoscandian Shield. Geological Society of America Special Papers 440, 229-248.

Korja, A., Kosunen, P., Heikkinen, P., 2009. A case study of lateral spreading: the Precambrian Svecofennian Orogen. Geological Society, London, Special Publications 321 (1), 225-251.

Korja, A., Lahtinen, R., Nironen, M., 2006. The Svecofennian orogen: a collage of microcontinents and island arcs. Geological Society, London, Memoirs 32 (1), 561-578.

Korja, T., 1993. Electrical conductivity distribution of the lithosphere in the central Fennoscandian Shield. Precambrian Res. 64 (1–4), 85-108.

Korsman, K., Koistinen, T., Kohonen, J., Wennerström, M., Ekdahl, E., Honkamo, M., Idman, H., Pekkala, Y., 1997. Bedrock map of Finland 1:1 000 000.

Korsman, K., Glebovitsky, V., 1999. Structure-lithology, metamorphism and metallogeny of the Raahe-Ladoga Zone. Special Maps- Geological Survey of Finland (Finland).

Korsman, K., Korja, T., Pajunen, M., Virransalo, P., GGT/SVEKA, W.G., 1999. The GGT/SVEKA Transect: Structure and Evolution of the Continental Crust in the Paleoproterozoic Svecofennian Orogen in Finland. Int. Geol. Rev. 41 (4), 287-333.

Kousa, J., Marttila, E., Vaasjoki, M., 1994. Petrology, geochemistry and dating of Paleoproterozoic metavolcanic rocks in the Pyhäjärvi area, central Finland. Geol.Surv.Finland, Special Paper 19, 7-27.

Koyi, H.A., Skelton, A., 2001. Centrifuge modelling of the evolution of low-angle detachment faults from high-angle normal faults. J. Struct. Geol. 23 (8), 1179-1185.

Kozlovskaya, E., Elo, S., Hjelt, S.-., Yliniemi, J., Pirttijärvi, M., 2004. 3-D density model of the crust of southern and central Finland obtained from joint interpretation of the SVEKALAPKO crustal P-wave velocity models and gravity data. Geophysical Journal International 158 (3), 827-848.

Kukkonen, I.T., Heikkinen, P., Ekdahl, E., Hjelt, S., Yliniemi, J., Jalkanen, E., FIRE Working Group., 2006. Acquisition and geophysical characteristics of reflection seismic data on FIRE transects, Fennoscandian Shield. Special Paper - Geological Survey of Finland 43 (Finnish Reflection Experiment FIRE 2001-2005), 13-30.

Kukkonen, I.T., Kuusisto, M., Lehtonen, M., Peltonen, P., 2008. Delamination of eclogitized lower crust: Control on the crust–mantle boundary in the central Fennoscandian shield. Tectonophysics 457 (3-4), 111-127.

Kuusisto, M., Kukkonen, I.T., Heikkinen, P., Pesonen, L.J., 2006. Lithological interpretation of crustal composition in the Fennoscandian Shield with seismic velocity data. Tectonophysics 420 (1-2), 283-299.

Lahtinen, R., 1994. Crustal evolution of the Svecofennian and Karelian domains during 2.1-1.79 Ga, with special emphasis on the geochemistry and origin of 1.93-1.91 Ga gneissic tonalites and associated supractustal rocks in the Rautalampi area, central Finland. Geological Survey of Finland, Bulletin 378, 1-128.

Lahtinen, R., Huhma, H., Lahaye, Y., Kousa, J., Luukas, J., 2015. Archean–Proterozoic collision boundary in central Fennoscandia: Revisited. Precambrian Res. 261, 127-165.

Lahtinen, R., Korja, A., Nironen, M., 2005. Chapter 11 Paleoproterozoic tectonic evolution. In: Lehtinen, M., Nurmi, P.A. and Rämö, O.T. (Eds.), Precambrian Geology of Finland Key to the Evolution of the Fennoscandian Shield.

Lahtinen, R., Huhma, H., 1997. Isotopic and geochemical constraints on the evolution of the 1.93-1.79 Ga Svecofennian crust and mantle in Finland. Precambrian Res. 82 (1–2), 13-34.

Lahtinen, R., Johnston, S.T., Nironen, M., 2014. The Bothnian coupled oroclines of the Svecofennian Orogen: a Palaeoproterozoic terrane wreck. Terra Nova 26 (4), 330-335.

Lahtinen, R., Korja, A., Nironen, M., Heikkinen, P., 2009. Palaeoproterozoic accretionary processes in Fennoscandia. Geological Society, London, Special Publications 318 (1), 237-256.

Lahtinen, R., Huhma, H., Lahaye, Y., Lode, S., Heinonen, S., Sayab, M., Whitehouse, M., 2016. Paleoproterozoic magmatism across the Archean-Proterozoic boundary in central Fennoscandia: Geochronology, geochemistry and isotopic data (Sm-Nd, Lu-Hf, O). Lithos 262, 507-525.

Leonov, M.G., 2012. Within-plate zones of concentrated deformation: Tectonic structure and evolution. Geotectonics 46 (6), 389-411.

Leonov, M.G., 2008. Lateral protrusions in the structure of the Earth´s lithosphere. Geotectonics 42 (5), 327-356.

Ludwig, K.R., 2003. Isoplot/Ex 3. A geochronological toolkit for Microsoft Excel. Berkeley Geochronology Center - Special publication 4.

Luosto, U., Heikkinen, P., 2001. Ylävaipan seismisestä rakenteesta Etelä-Suomessa. Geophysical Society of Finland 20, 117-5.

Meissner, R., Tilmann, F., Haines, S., 2004. About the lithospheric structure of central Tibet, based on seismic data from the INDEPTH III profile. Tectonophysics 380 (1–2), 1-25.

Molnar, P., Tapponnier, P., 1977. Relation of the tectonics of eastern China to the India-Eurasia collision: Application of slip-line field theory to large-scale continental tectonics. Geology} 5 (4), 212-216.

Mooney, W.D., 2015. 1.11 - Crust and Lithospheric Structure - Global Crustal Structure. In: Schubert, G. (Ed.), Treatise on Geophysics (Second Edition). Elsevier, Oxford.

Mooney, W.D., Laske, G., Masters, T.G., 1998. CRUST 5.1: A global crustal model at 5° × 5°. Journal of Geophysical Research: Solid Earth 103 (B1), 727-747.

Nelson, K.D., Zhao, W., Brown, L.D., Kuo, J., Che, J., Liu, X., Klemperer, S.L., Makovsky, Y., Meissner, R., Mechie, J., Kind, R., Wenzel, F., Ni, J., Nabelek, J., Leshou, C., Tan, H., Wei, W., Jones, A.G., Booker, J., Unsworth, M., Kidd, W.S.F., Hauck, M., Alsdorf, D., Ross, A., Cogan, M., Wu, C., Sandvol, E., Edwards, M., 1996. Partially Molten Middle Crust Beneath Southern Tibet : Synthesis of Project INDEPTH Results. Science 274, 1684-1687.

Nemčok, M., Mora, A., Cosgrove, J., 2013. Thick-skin-dominated orogens; from initial inversion to full accretion: an introduction. Geological Society, London, Special Publications 377 (1), 1-17.

Nikkilä, K., Roy Chowdhury, B.S., Dietl, C., Korja, A., Eklund, O., Zanella, F., 2009. Thermomechanical analogue modelling of the extensional collapse of a collisional orogeny the Svecofennian orogen, Finland. Geotectonic Research 96, 21-38.

Nikkilä, K., Korja, A., Koyi, H., Eklund, O., 2015. Analog modeling of one-way gravitational spreading of hot orogens – A case study from the Svecofennian orogen, Fennoscandian Shield. Precambrian Res. 268, 135-152.

Nikkilä, K., Mänttäri, I., Nironen, M., Eklund, O., Korja, A., 2016. Three stages to form a large batholith after terrane accretion – An example from the Svecofennian orogen. Precambrian Res. 281, 618-638.

Nironen, M., Elliott, B., Rämö, O., 2000. 1.88–1.87 Ga post-kinematic intrusions of the Central Finland Granitoid Complex: a shift from C-type to A-type magmatism during lithospheric convergence. Lithos 53 (1), 37-58.

Nironen, M., Lahtinen, R., Koistinen, T., 2002. Suomen geologiset aluenimet–yhtenäisempään nimikäytäntöön. Summary: Subdivision of Finnish bedrock–an attempt to harmonize terminology. Geologi 54 (1), 8-14.

Nironen, M., 2003. Keski-Suomen granitoidikompleksi–kallioperäkartan selitys. Geological Survey of Finland - Report of Investigation 157, 1-45.

Paavola, J., 1988. Lapinlahden kartta-alueen kallioperä. Kallioperäkartan selitys 1 : 100 000 - Expl. to Maps of Pre-Quat. Rocks .

Paavola, J., 1987. Lapinlahti. Kallioperäkartta 1:100 000 - Maps of Pre-Quaternary Rocks.

Paterson, S.R., Miller, R.B., 1998. Magma emplacement during arc-perpendicular shortening: An example from the Cascades crystalline core, Washington. Tectonics 17 (4), 571-586.

Petford, N., Cruden, A.R., McCaffrey, K.J.W., Vigneresse, J.-., 2000. Granite magma formation, transport and emplacement in the Earth's crust. Nature 408 (6813), 669-673.

Rämö, O.T., Vaasjoki, M., Mänttäri, I., Elliott, B.A., Nironen, M., 2001. Petrogenesis of the Post-kinematic Magmatism of the Central Finland Granitoid Complex I; Radiogenic Isotope Constraints and Implications for Crustal Evolution. Journal of Petrology 42 (11), 1971-1993.

Ranalli, G., 2000. Rheology of the crust and its role in tectonic reactivation. Journal of Geodynamics 30 (1–2), 3-15.

Rasilainen, K., Lahtinen, R., Bornhorst, T.J., 2007. The rock geochemical database of Finland manual. Geological Survey of Finland - Report of Investigation (Electronic resource) (164), 1-38.

Rey, P., Vanderhaeghe, O., Teyssier, C., 2001. Gravitational collapse of the continental crust: definition, regimes and modes. Tectonophysics 342 (3–4), 435-449.

Rey, P.F., Coltice, N., 2008. Neoarchean lithospheric strengthening and the coupling of Earth's geochemical reservoirs. Geology 36 (8), 635-638.

Ries, A.C., Shackleton, R.M., 1976. Patterns of Strain Variation in Arcuate Fold Belts. Philosophical Transactions of the Royal Society of London A: Mathematical, Physical and Engineering Sciences 283 (1312), 281-288.

Rosenberg, C.L., Handy, M.R., 2005. Experimental deformation of partially melted granite revisited: implications for the continental crust. J. Metamorph. Geol. 23 (1), 19-28.

Royden, L., 1996. Coupling and decoupling of crust and mantle in convergent orogens; implications for strain partitioning in the crust. Journal of Geophysical Research 101 (B8), 17-17,705.

Royden, L.H., Burchfiel, B.C., van der Hilst, R.D., 2008. The Geological Evolution of the Tibetan Plateau. Science 321 (5892), 1054-1058.

Ruotoistenmäki, T., Mänttäri, I., Paavola, J., 2001. Characteristics of Proterozoic late-/post-collisional intrusives in Archaean crust in Iisalmi-Lapinlahti area, Central Finland. Special Paper - Geological Survey of Finland, 105-116.

Rutter, E.H., 1997. The influence of deformation on the extraction of crustal melts: a consideration of the role of melt-assisted granular flow. In: Holness, M.B. (Ed.), Deformation-Enhanced Fluid Transport in the Earth's Crust and Mantle. Chapman & Hall, London.

Scheuber, E., Gonzalez, G., 1999. Tectonics of the Jurassic-Early Cretaceous magmatic arc of the north Chilean Coastal Cordillera (22°–26°S): A story of crustal deformation along a convergent plate boundary. Tectonics 18 (5), 895-910.

Selonen, O., Ehlers, C., 1996. The Orivesi granite batholith, Southern Central Finland-characteristics and emplacement. Bulletin-Geological Society of Finland 68, 11-24.

Shapiro, N.M., Ritzwoller, M.H., Molnar, P., Levin, V., 2004. Thinning and Flow of Tibetan Crust Constrained by Seismic Anisotropy. Science 305, 233-236.

Solar, G.S., Pressley, R.A., Brown, M., Tucker, R.D., 1998. Granite ascent in convergent orogenic belts: testing a model. Geology 26 (8), 711-714.

Sorjonen-Ward, P., Luukkonen, E.J., 2005. Chapter 2 Archean rocks. Developments in Precambrian Geology, Elsevier 14, 19-99.

Sorjonen-Ward, P., 2006. Geological and structural framework and preliminary interpretation of the FIRE 3 and FIRE 3A reflection seismic profiles, central Finland. Special Paper - Geological Survey of Finland 43, 105-159.

Sorjonen-Ward, P., 2003. Outokumpu Mineralising System: Geological Interpretation. CSIRO Exploration and Mining Report 1143C, 215.

Tapponnier, P., Peltzer, G., Le Dain, A.Y., Armijo, R., Cobbold, P., 1982. Propagating extrusion tectonics in Asia: New insights from simple experiments with plasticine. Geology 10 (12), 611-616.

Teng, L.S., 1996. Extensional collapse of the northern Taiwan mountain belt. Geology 24 (10), 949-952.

Tetreault, J.L., Buiter, S.J.H., 2014. Future accreted terranes: a compilation of island arcs, oceanic plateaus, submarine ridges, seamounts, and continental fragments. Solid Earth 5, 1243-1275.

Tetreault, J.L., Buiter, S.J.H., 2012. Geodynamic models of terrane accretion: Testing the fate of island arcs, oceanic plateaus, and continental fragments in subduction zones. Journal of Geophysical Research: Solid Earth 117 (B8), n/a-n/a.

Torvela, T., 2016. How (not) to recognize mid-crustal channel flow from outcrop patterns. Geological Society of America, Special Publication .

Torvela, T., Moreau, J., Butler, R.W.H., Korja, A., Heikkinen, P., 2013. The mode of deformation in the orogenic mid-crust revealed by seismic attribute analysis. Geochem. Geophys. Geosyst. 14 (4), 1069-1086.

Vaarma, M., Pipping, F., 2003. Kyyjärvi - Perho kartta-alueen kallioperä. Geological map of Finland,1 : 100 000, Explanation to the maps of Pre-Quaternary rocks 2331; 2332.

Väisänen, M., Mänttäri, I., Hölttä, P., 2002. Svecofennian magmatic and metamorphic evolution in southwestern Finland as revealed by U-Pb zircon SIMS geochronology. Precambrian Res. 116 (1–2), 111-127.

Vanderhaeghe, O., Burg, J., Teyssier, C., 1999. Exhumation of migmatites in two collapsed orogens: Canadian Cordillera and French Variscides. Geological Society, London, Special Publications 154 (1), 181-204.

Vanderhaeghe, O., 2009. Migmatites, granites and orogeny: Flow modes of partially-molten rocks and magmas associated with melt/solid segregation in orogenic belts. Tectonophysics 477 (3–4), 119-134.

Vanderhaeghe, O., Teyssier, C., 2001. Partial melting and flow of orogens. Tectonophysics 342 (3-4), 451-472.

Vernon, R.H., 2000. Review of Microstructural Evidence of Magmatic and Solid-State Flow. Visual Geosciences 5 (2), 1-23.

Vigneresse, J.L., 1995. Crustal regime of deformation and ascent of granitic magma. Tectonophysics 249 (3–4), 187-202.

Weil, A.B., Gutiérrez-Alonso, G., Johnston, S.T., Pastor-Galán, D., 2013. Kinematic constraints on buckling a lithospheric-scale orocline along the northern margin of Gondwana: A geologic synthesis. Tectonophysics 582, 25-49.

Whitehouse, M.J., Kamber, B., Moorbath, S., 1999. Age significance of U–Th–Pb zircon data from early Archaean rocks of west Greenland – a reassessment based on combined ion-microprobe and imaging studies. Chemical Geology 160, 201-224.

Whitehouse, M.J., Kamber, B.S., 2005. Assigning Dates to Thin Gneissic Veins in High-Grade Metamorphic Terranes: A Cautionary Tale from Akilia, Southwest Greenland. Journal of Petrology 46, 291-318.

Whitney, D.L., Teyssier, C., Vanderhaeghe, O., 2004. Gneiss domes and crustal flow. Geological Society of America Special Papers 380, 15-33.

Willett, S.D., 1999. Rheological dependence of extension in wedge models of convergent orogens. Tectonophysics 305 (4), 419-435.

Zhao, G., Sun, M., Wilde, S.A., Li, S., 2004. A Paleo-Mesoproterozoic supercontinent: assembly, growth and breakup. Earth-Sci. Rev. 67 (1–2), 91-123.

Ziegler, P.A., van Wees, J., Cloetingh, S., 1998. Mechanical controls on collision-related compressional intraplate deformation. Tectonophysics 300 (1–4), 103-129.

ISBN 978-952-12-3429-3
Åbo Akademi